



Human retinal pigment epithelial cells prefer proline as a nutrient and transport metabolic intermediates to the retinal side

Received for publication, March 27, 2017, and in revised form, May 30, 2017. Published, Papers in Press, June 14, 2017, DOI 10.1074/jbc.M117.788422

Jennifer R. Chao^{†1}, Kaitlen Knight[‡], Abbi L. Engel[‡], Connor Jankowski[§], Yekai Wang^{¶||}, Megan A. Manson[‡], Haiwei Gu^{**}, Danijel Djukovic^{**}, Daniel Raftery^{**}, James B. Hurley^{‡§}, and Jianhai Du^{¶||2}

From the Departments of [†]Ophthalmology and [§]Biochemistry and ^{**}Northwest Metabolomics Research Center, Department of Anesthesiology and Pain Medicine, University of Washington, Seattle, Washington 98109 and the Departments of [¶]Ophthalmology and ^{||}Biochemistry, West Virginia University, Morgantown, West Virginia 26506

Edited by Paul E. Fraser

Metabolite transport is a major function of the retinal pigment epithelium (RPE) to support the neural retina. RPE dysfunction plays a significant role in retinal degenerative diseases. We have used mass spectrometry with ¹³C tracers to systematically study nutrient consumption and metabolite transport in cultured human fetal RPE. LC/MS-MS detected 120 metabolites in the medium from either the apical or basal side. Surprisingly, more proline is consumed than any other nutrient, including glucose, taurine, lipids, vitamins, or other amino acids. Besides being oxidized through the Krebs cycle, proline is used to make citrate via reductive carboxylation. Citrate, made either from ¹³C proline or from ¹³C glucose, is preferentially exported to the apical side and is taken up by the retina. In conclusion, RPE cells consume multiple nutrients, including glucose and taurine, but prefer proline, and they actively synthesize and export metabolic intermediates to the apical side to nourish the outer retina.

The retinal pigment epithelium (RPE)³ in the vertebrate eye is a monolayer of polarized pigmented epithelial cells that is situated between the photoreceptors and the choroidal blood supply. The RPE provides critical support for the function of the neural retina. It has many long microvilli at its apical side that wrap around the photoreceptor outer segments. On its basal side, the RPE forms convoluted microinfolds that increase its surface area. It transports nutrients and metabolites, recycles

retinoids, and engulfs shed outer segment (1, 2). Failure of the RPE leads to photoreceptor degeneration in diseases including age-related macular degeneration (AMD), bestrophinopathy, and Sorsby fundus dystrophy (3–7).

A major function of the RPE is to transport metabolites between the choroid and retina. Photoreceptors have a high demand for energy and are highly glycolytic; like many cancer cells, they metabolize about 90% of the glucose they consume into lactate (8, 9). RPE cells directionally transport glucose to the retina and lactate into the blood through highly expressed glucose transporters and monocarboxylate transporters on both the apical and basal membranes (1, 10, 11). Loss of monocarboxylate transporters causes retinal dysfunction and degeneration (12, 13). However, less is known about the transport of other nutrients and metabolites through the RPE.

The RPE requires an active metabolism to support its multiple functions. Either suppression of its mitochondrial metabolism or activation of glycolysis can cause RPE dysfunction to induce an AMD-like phenotype in mouse models (14, 15). How the RPE imports nutrients to support its own energy demands is still unclear.

Human fetal RPE (hFRPE) cultures have similar morphological and physiological characteristics as native RPE (16). These cultures have been well-characterized as a useful model for evaluating RPE metabolism (17) and RPE diseases, including AMD (18). The RPE cultures used in the experiments conducted in this manuscript are of a similar age in culture as the ones used in studies published previously, including investigations of the cause of AMD.

MS provides a sensitive, quantitative, and high-throughput platform to measure metabolites. Transport of metabolites labeled with a stable isotope and biochemical transformations of those metabolites can be monitored. In this report, we use both LC/MS-MS and GC-MS coupled with ¹³C metabolic flux analysis to investigate how nutrients are consumed and how metabolites are transported through cultured hFRPE cells. Surprisingly, we found that proline is the most preferred fuel for RPE cells. They convert proline into ornithine and mitochondrial intermediates through multiple mitochondrial pathways. We also found that RPE transports metabolic intermediates, including citrate, glutamate, serine, and glycine, to its apical side and that, when these metabolites are released from the

This work was supported by National Institutes of Health Grants EY026030 (to J. D., J. B. H., and J. R. C.), EY06641 and EY017863 (to J. B. H.), and EY019714 (to J. R. C.) and the Brightfocus Foundation (to J. D. and J. R. C.). The authors declare that they have no conflicts of interest with the contents of this article. The content is solely the responsibility of the authors and does not necessarily represent the official views of the National Institutes of Health. This article contains supplemental Experimental Procedures, Figs. 1–4, and Tables 1–3.

¹ To whom correspondence may be addressed: 750 Republican St., Box 358058, Seattle, WA 98109. Tel.: 206-221-0594; E-mail: jrchoa@uw.edu.

² To whom correspondence may be addressed: 1 Medical Center Dr., P. O. Box 9193, WVU Eye Institute, Morgantown, WV 26505. Tel.: 304-598-6903; Fax: 304-598-6928; E-mail: jianhai.du@wvumedicine.org.

³ The abbreviations used are: RPE, retinal pigment epithelium; AMP, age-related macular degeneration; hFRPE, human fetal retinal pigment epithelium; TCA, tricarboxylic acid; P5C, pyrroline-5-carboxylate; KRB, Krebs-Ringer bicarbonate buffer; α KG, α -ketoglutarate; OAT, ornithine aminotransferase; ECM, extracellular matrix; TER, transepithelial resistance.

Metabolite transport in RPE

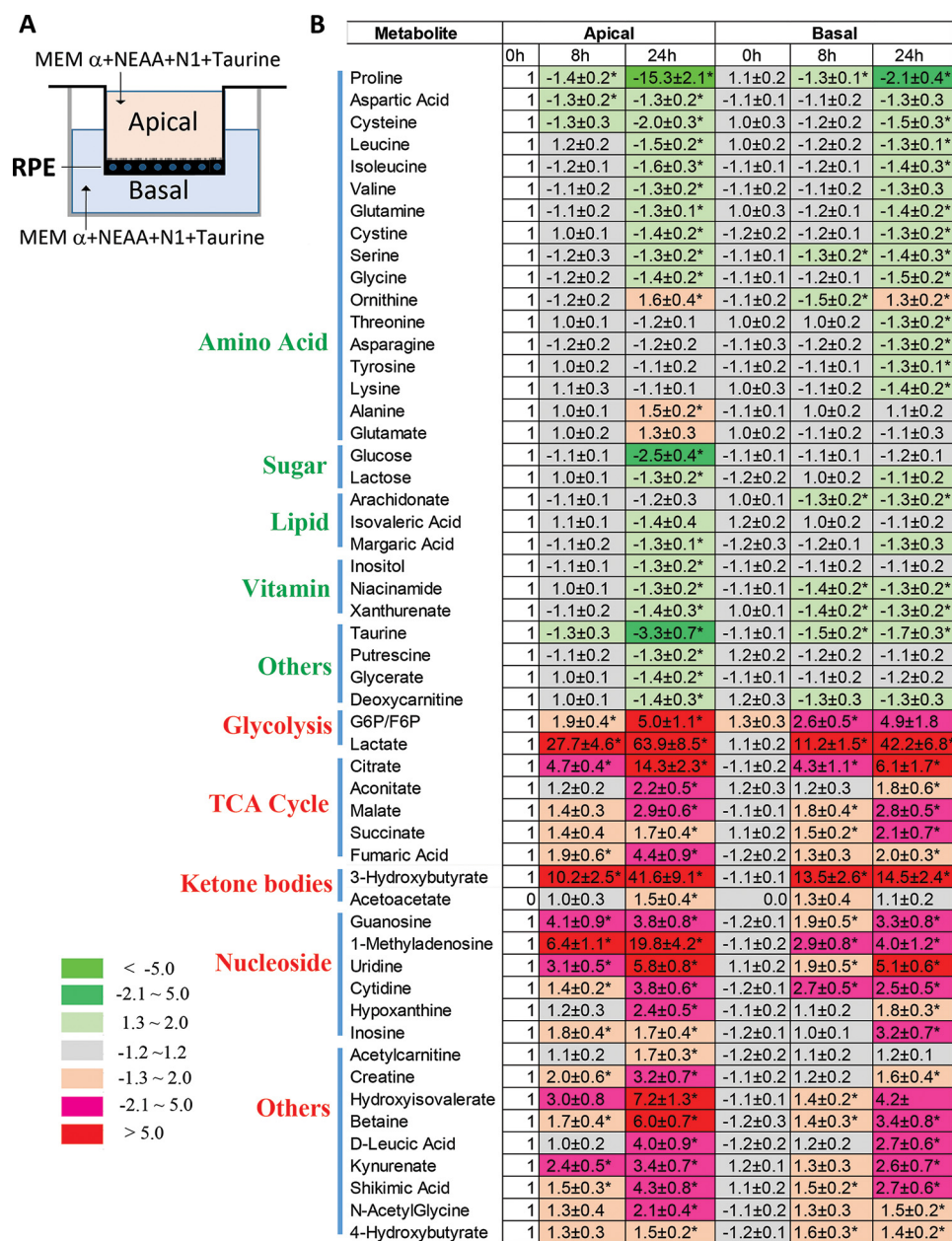


Figure 1. The nutrient consumption of hRPE cells from the apical and basal sides. A, schematic illustrating hRPE cultured on transwell filter membranes with 500 μ l of RPE medium on each side. MEM α , minimum Eagle's medium α . B, metabolite consumption and generation in RPE. 40 μ l of medium was sampled from each side at different time points, and metabolites were analyzed by LC/MS-MS. Green represents consumed metabolites, and red represents generated metabolites. Data are the average -fold change \pm S.D. over the intensity at 0 h from the apical side with the exception of acetoacetate. Acetoacetate is undetectable at 0 h, and its change is represented as -fold over intensity at 8 h from the apical side. *, $p < 0.05$ versus 0 h control ($n = 4$).

apical RPE, they can be taken up by the retina. We report here a comprehensive study of nutrient utilization and metabolite transport in RPE. Our findings provide new insights into RPE biochemistry and physiology and its role in the pathogenesis of retinal diseases, including AMD.

Results

RPE preferentially consumes proline, glucose, and taurine, and it exports metabolic intermediates from both its apical and basal surfaces

To examine how the RPE consumes and metabolizes nutrients, we cultured hRPE cells on filter membrane inserts (Fig. 1A) and quantified metabolites in RPE culture medium from

both the apical and basal chambers 0, 8, and 24 h after changing the culture to fresh medium (Fig. 1B). RPE cells cultured on filter inserts developed the polarity seen in native tissue, including apical microvilli, basal infoldings, and tight junctions, as seen by transmission electron microscopy (supplemental Fig. 1). For these experiments, we used a rich RPE medium containing all 20 amino acids, glucose, taurine, pyruvate, and other supplements (the formulation is listed in supplemental Table 1). We quantified 202 metabolites, covering most major metabolic pathways, and detected 110 metabolites in the medium (supplemental Table 2). Of these metabolites, 53 changed substantially between 0 and 8 h (-fold change > 1.3 or < -1.3) (Fig. 1B). Surprisingly, more proline was consumed than any of the

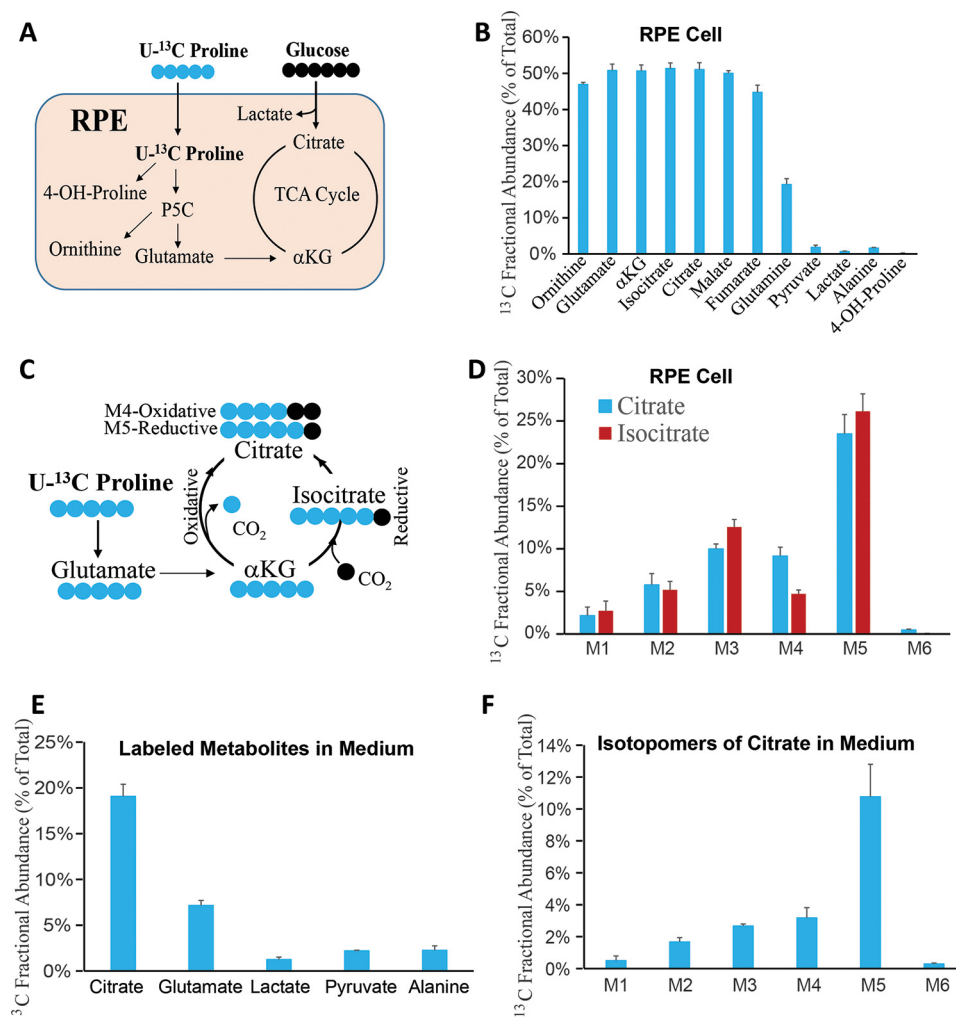


Figure 2. Proline is utilized to generate intermediates through both mitochondrial oxidative and reductive pathways. *A*, schematic of tracing proline metabolism in RPE cells. hRPE cells were grown in 6-well plates and incubated with [U-¹³C]proline (¹³C carbon in blue) and glucose (¹²C carbon in black). *B*, [U-¹³C]proline-labeled metabolites in hRPE. hRPE cells were incubated with 2 mM [U-¹³C]proline in the presence of 5 mM glucose in KRB for 1 h. *C*, schematic of mitochondrial oxidative and reductive pathways. Shown in blue is ¹³C (labeled), and shown in black is ¹²C (unlabeled). *D*, [U-¹³C]proline labeled both oxidative and reductive pathways. M4 citrate/isocitrate derives from the oxidative pathway, and M5 citrate/isocitrate derives from the reductive pathway. *E* and *F*, [U-¹³C]proline-labeled intermediates that are exported into the medium ($n = 3$).

other metabolites we measured. After 24 h, the amount of proline decreased 15.3-fold on the apical side and 2.1-fold on the basal side. As expected, RPE also consumed substantial amounts of glucose (−2.5) and taurine (−3.3). Other metabolites decreased by less than −2-fold. Nutrients in the medium were consumed through multiple pathways, including the tricarboxylic acid (TCA), β -oxidation, ketogenesis, and pentose phosphate pathways. Intermediates in those pathways accumulated in the medium at 8 and 24 h. For example, lactate, 3-hydroxybutyrate, citrate, and 1-methyladenosine increased >10-fold on the apical side (Fig. 1*B*). In general, these intermediates increased earlier and more substantially on the apical side compared with the basal side, suggesting that RPE may actively transport these metabolites. To exclude the influence of filter coating on metabolite transport, we quantified the ratios of metabolites from the two sides from wells with coated inserts without RPE after 24-h incubation. The metabolites reached equilibrium with ratios between the two sides of less than 1.2 (supplemental Table 3).

Proline is converted into ornithine and TCA cycle intermediates through both oxidative and reductive pathways

To determine how proline is metabolized, we used [U-¹³C]proline to trace its metabolism through known pathways. For example, proline can be reduced to form pyrroline-5-carboxylate (P5C). P5C can be converted into ornithine or glutamate, which can feed into the TCA cycle (Fig. 2*A*). To avoid interference from other nutrient sources, we changed the medium to KRB containing only 5 mM glucose and 2 mM [U-¹³C]proline. After 1 h, the intensity of [U-¹³C]proline dropped 20% in the medium (supplemental Fig. 2), consistent with our finding that RPE cells prefer proline. Even in the presence of unlabeled glucose, about half of the pool of ornithine, glutamate, and TCA cycle intermediates was labeled with ¹³C from [U-¹³C]proline (Fig. 2*B*). Only ~5% of pyruvate, alanine, and lactate become labeled, possibly through malic enzyme activity. Proline can also be hydroxylated to form hydroxyproline. However, we did not detect any [¹³C]hydroxyproline

Metabolite transport in RPE

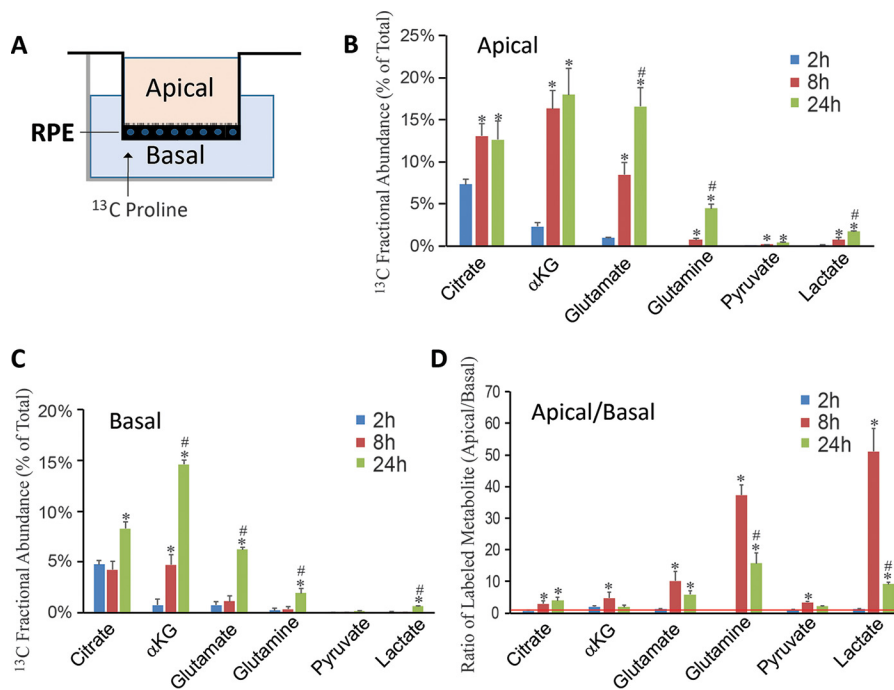


Figure 3. Proline is consumed to generate intermediates on both the apical and basal sides. A, schematic illustrating hFrPE cells with [U-¹³C]proline added to the basal side. hFrPE was cultured on filter membrane inserts with 500 μ l of DMEM containing 5.5 mM glucose and 1% FBS on each side. B and C, ¹³C-labeled intermediates in the medium from the apical and basal sides. D, the distribution of [¹³C]proline-labeled intermediates on the apical compared with the basal side. The data are represented as the ratio of the intensity of labeled metabolites from the apical side to that of the basal side. The red line represents an even distribution (ratio = 1). *, $p < 0.05$ versus 2-h control; #, $p < 0.05$ versus 8-h control ($n = 3$).

after 1 h, indicating that free proline may not be hydroxylated into hydroxyproline or that hydroxyproline turnover is slow.

Recently, we reported that reductive carboxylation is a major metabolic pathway in RPE cells (19). When [U-¹³C]proline is used to generate citrate by reductive carboxylation, all five carbons from citrate are labeled with ¹³C (M5); if it goes through the classic TCA cycle, then one carbon is removed by decarboxylation catalyzed by α -ketoglutarate (α KG) dehydrogenase, so the citrate produced is M4 (Fig. 2C). We found that M5 citrate/isocitrate is the predominant isotopomer after 1-h labeling of hFrPE cells with [¹³C]proline. M5 citrate is 2.5-fold more enriched than M4 citrate/isocitrate (Fig. 2D). The M3 and M2 isotopomers are derivatives of M5 and M4, respectively, after a second round of reactions after citrate lyase. Proline-derived citrate and other intermediates are exported into the medium (Fig. 2E). M5 citrate also is the predominant isotopomer in the medium (Fig. 2F).

RPE exports proline-derived intermediates preferentially to the apical side

We evaluated the fate of metabolites derived from proline by incubating hFrPE on transwell filters with [U-¹³C]proline in DMEM with glucose and 1% FBS on the basal side of the filter (Fig. 3A). The enrichment of intermediates with ¹³C increased from 2 h on both the apical and basal sides and reached its highest point at 24 h (Fig. 3, B and C). The metabolites on the apical side increased more substantially at 8 h (Fig. 3D), but the differences between apical and basal levels were somewhat smaller by 24 h.

RPE exports glucose-derived intermediates preferentially to the apical side

Glucose is considered to be an essential nutrient source for RPE (20). We confirmed this by showing that glucose is consumed significantly in hFrPE culture (Fig. 1B). To study how intermediates derived from glucose are exported from RPE cells, we added [U-¹³C]glucose at either the apical or basal side with unlabeled glucose on the opposite side and quantified the labeled intermediates from both sides at 8, 24, and 48 h (Fig. 4, A and E). GC-MS data showed a time-dependent increase of intermediates from glucose metabolism in the medium from both apical and basal sides. Lactate, pyruvate, alanine, serine, and glycine are generated from glycolysis, and citrate, malate, glutamate, and glutamine are from the mitochondrial TCA cycle (Fig. 4 and supplemental Fig. 3). When [¹³C]glucose is added to the apical side, the apical intermediates reach a steady state by 24 h, whereas accumulation of most intermediates on the basal side is delayed (Fig. 4, B and C). The concentration difference of labeled metabolites between apical and basal compartments was highest at 8 h, with ~10-fold more on the apical side (Fig. 4D). When [¹³C]glucose is provided on the basal side (Fig. 4E), intermediates were labeled more slowly with lower enrichment. The concentration difference also is less obvious for most intermediates, with the exception of glutamine (Fig. 4, F–H). Serine and glycine labeled with ¹³C also are exported (supplemental Fig. 3). Because there were high concentrations of unlabeled serine and glycine (0.4 mM) in the DMEM, the apparent enrichment of serine and glycine was diluted to less than 5%. Remarkably, no matter the side to which [¹³C]glucose was added, citrate, glutamate, and glutamine were at higher

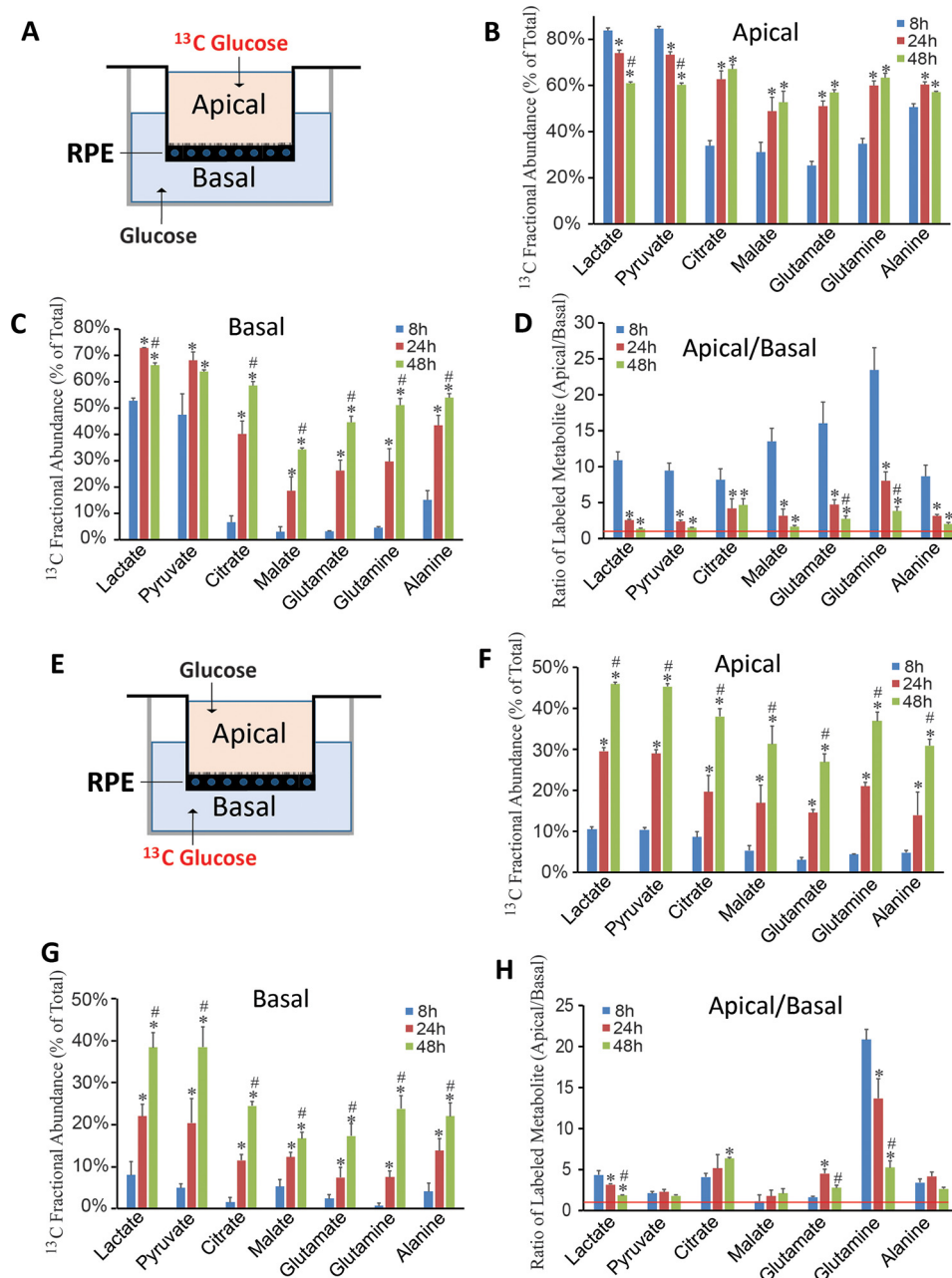


Figure 4. Distribution of glucose-derived intermediates on the apical and basal sides. *A* and *E*, schematic illustrating hRPE cultured on filter membrane inserts with 500 μ l of DMEM containing 2 mM glutamine and 1% FBS on each side. 5.5 mM [^{13}C]glucose was added to either the apical side (*A*) or the basal side (*E*), and 5.5 mM unlabeled glucose was added to the contralateral side. *B*, *C*, *F*, and *G*, ^{13}C -labeled intermediates in medium from the apical and basal side after 8, 24, and 48 h. *D* and *H*, the distribution of [^{13}C]glucose-labeled intermediates on the apical compared with the basal side. The data are represented as the ratio of the intensity of labeled metabolites from the apical side to that of the basal side. The red line represents even distribution (ratio = 1). *, $p < 0.05$ versus 8-h control; #, $p < 0.05$ versus 24-h control ($n = 3$).

levels on the apical side than on the basal side, suggesting that export of these metabolites can supply energy to the outer retina.

Mitochondrial function enhances transport of some metabolic intermediates

We noted that mitochondrial intermediates are exported into the medium. To test the importance of mitochondrial energy metabolism in metabolite transport, we used rotenone to block mitochondrial respiratory complex I in hRPE cells (Fig. 5*A*). When complex I (NADH dehydrogenase) is inhibited,

NADH should accumulate in the mitochondrial matrix. Malate can be exported to the cytoplasm, where its reducing power can be transferred through NADH to convert pyruvate to lactate. Pyruvate is drawn away from entering mitochondria, and oxaloacetate is drawn out of the matrix as malate. Together, these would decrease the matrix concentrations of the substrates for synthesizing citrate (Fig. 5*A*). Consistent with this interpretation, we found that 8 h of rotenone treatment caused relative increases of lactate and malate and a relative decrease of pyruvate and citrate. We noted that glycine and serine decreased more substantially on the basal side (Fig. 5, *B* and *C*). We also noted

Metabolite transport in RPE

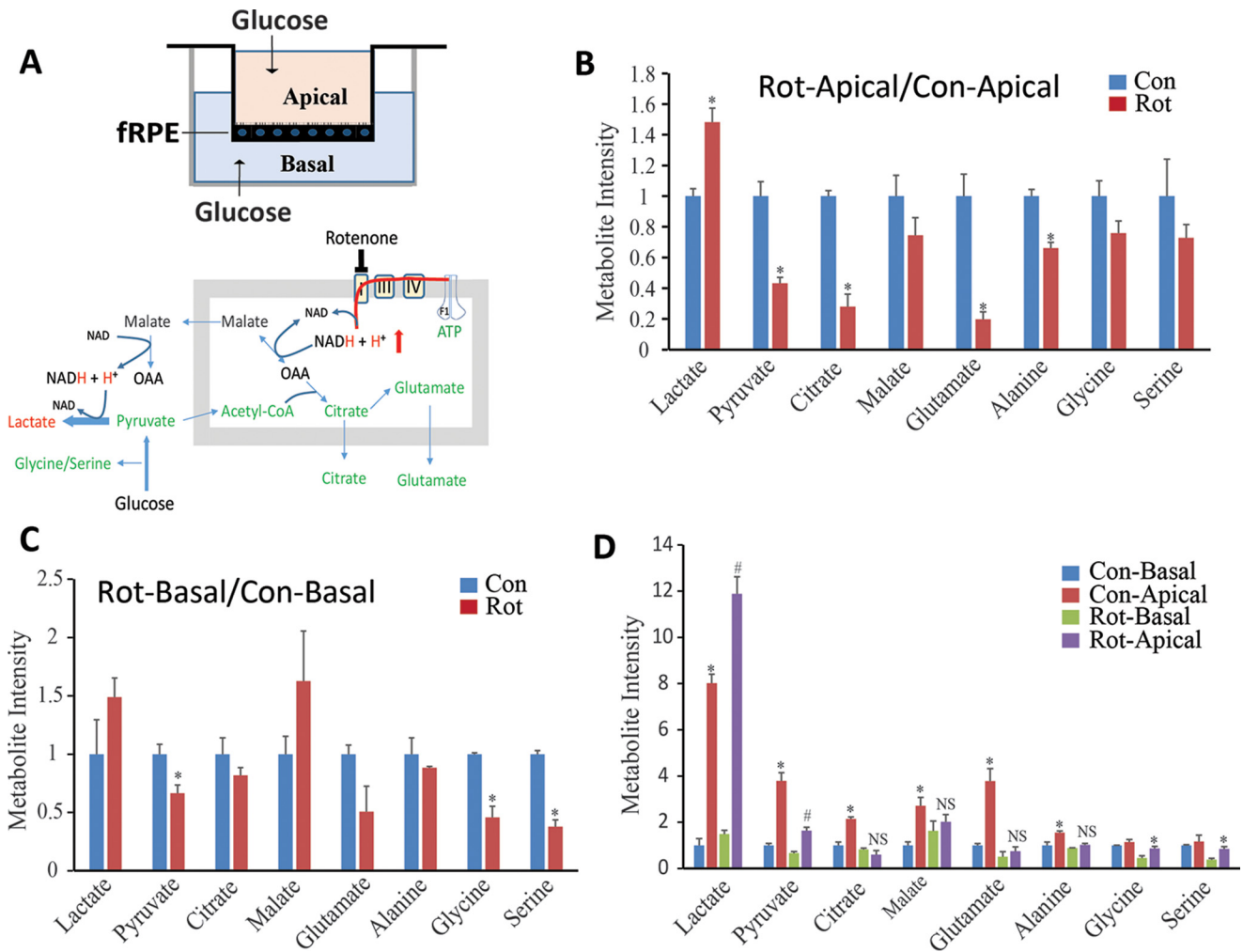


Figure 5. Mitochondrial function is essential for metabolite export. *A*, top panel, schematic illustrating hRPE culture on filter membrane inserts with medium containing 5.5 mM glucose and 2 mM glutamine in DMEM with 1% FBS in both apical and basal chambers. Bottom panel, schematic of how inhibition of mitochondrial complex I with rotenone redistributes the redox from mitochondria to the cytosol and impacts metabolite levels. Red denotes an increase, and green denotes a decrease. *B–D*, inhibition of mitochondrial complex I by treatment with rotenone for 8 h. The data are represented as the -fold change of metabolite intensity with rotenone treatment over the untreated control on the apical side (*B*) and basal side (*C*). *D*, data are represented as the -fold change of metabolite intensity in the basal compartment of untreated controls. *, $p < 0.05$ versus control on the apical or basal side; #, $p < 0.05$ versus rotenone on the apical or basal side; NS, no significance ($n = 3$).

that inhibition of mitochondrial metabolism abrogated the apical preference for citrate, malate, glutamate, and alanine (Fig. 5D). To monitor cell death, we tested the release of lactate dehydrogenase from the cells into the medium. There was little evidence of cell death in these experiments (supplemental Fig. 4).

The retina imports metabolites exported by the RPE

To determine whether metabolites from the RPE can be imported as nutrients by the retina, we co-cultured mouse retina with photoreceptors in contact with the apical side of RPE cells grown on transwell filters. We then added [^{13}C]glucose to the basal side (Fig. 6A). The retina has a high rate of aerobic glycolysis that metabolizes glucose to lactate. As expected, the retina enhanced accumulation of labeled lactate in both the apical and basal chambers. The retina caused depletion of both citrate and glutamate from the apical medium, indicating that they were taken up by the retina. Glutamine accumulated on the apical side but decreased on the basal side. Labeled serine and glycine were depleted only on the basal side (Fig. 6, B and

C). To examine how retina co-culture affected RPE metabolism, we quantified the intracellular metabolites in RPE cells. Only lactate was increased in RPE cells co-cultured with retina, supporting the idea that RPE imports retina-derived lactate. These results suggest that the retina does not significantly affect intracellular glucose metabolism in RPE under these conditions (Fig. 6D).

To further examine whether metabolites released into the medium by RPE cells are used by the retina, we compared labeled metabolites in retina from [^{13}C]glucose with or without RPE. Strikingly, co-culture with RPE markedly increased lactate, pyruvate, citrate, αKG , alanine, glutamine, serine, and glycine (Fig. 6E), corroborating our hypothesis that RPE exports intermediates to support the retina (Fig. 6F).

Discussion

RPE culture is an excellent *in vitro* model to study RPE function and AMD (17, 21). In this study, we used targeted metabolomics to study how the RPE consumes nutrients. Unexpect-

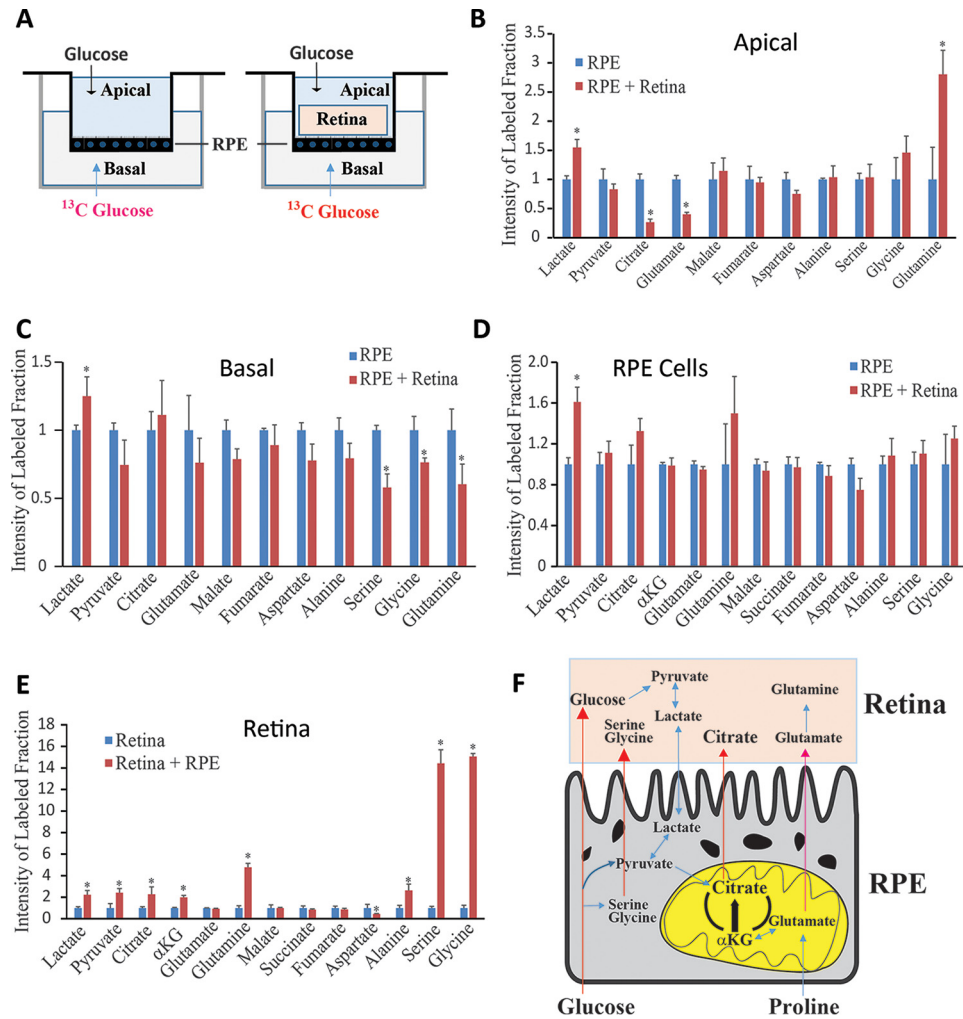


Figure 6. Retina uptake of the metabolites released by RPE. *A*, top panel, schematic illustrating hRPE cultured on filter inserts with and without mouse retina overlay. The medium consisted of DMEM with 1% FBS and 2 mM glutamine with unlabeled 5.5 mM glucose on the apical side and 5.5 mM [U- ^{13}C]glucose on the basal side. *B* and *C*, the intensity of labeled metabolites in apical or basal medium. *, $p < 0.05$ versus RPE cells only ($n = 3$). *D*, the intensity of labeled metabolites in RPE cells. *, $p < 0.05$ versus RPE cells only ($n = 3$). *E*, the intensity of labeled metabolites in mouse retina. Mouse retina was incubated with [U- ^{13}C]glucose with or without RPE cells. *, $p < 0.05$ versus retina only ($n = 3$). *F*, schematic of metabolite transport between the RPE and retina.

edly, we found that RPE cells prefer proline as an energy substrate. We also developed a stable isotope-based approach to trace metabolite transport out of the RPE to either its apical or its basal side, and we showed that metabolites exported from the RPE can support retinal metabolism.

Proline is consumed by RPE cells faster than any other nutrients in the culture medium. Proline is a non-essential amino acid that is not normally included in standard DMEM preparations. However, proline ranging from 10–115 mg/liter is typically included in most of the widely used protocols for human RPE culture media (16, 21–27). Proline can be provided within the RPE by synthesis either from glutamate by P5C synthase or from ornithine by ornithine aminotransferase (OAT). Deficiency of OAT can cause gyrate atrophy, an inborn error of metabolism characterized by lobular loss of RPE and choroid (28, 29). RPE has been identified as the major and most early damaged site in gyrate atrophy (29). Intriguingly, supplementation with proline rescues ornithine cytotoxicity induced by inhibition of OAT in RPE cells (30, 31). Under our experimental conditions, glutamate and arginine (the precursor of ornithine)

are not significantly used in 24 h (Fig. 1*B*), indicating that proline in RPE cells is more dependent on exogenous supply.

Proline imported into RPE cells can be catabolized into glutamate for mitochondrial intermediates and into ornithine for urea cycle activity. We found that ^{13}C from proline replaced 50% of the endogenous glutamate, ornithine, and mitochondrial intermediates within 1 h (Fig. 2*B*). Labeled glutamate and ornithine accumulated at 24 h, even in the presence of abundant glutamate, glutamine, and arginine in the RPE culture medium (Fig. 2*B*). These results demonstrate that proline is an important nutrient source for RPE metabolism. In addition to being oxidized through the TCA cycle, proline fuels the active reductive carboxylation pathway we reported previously in RPE cells (19). Reductive carboxylation increases mitochondrial bioenergetics and cellular resistance against oxidative damage. Both mitochondrial dysfunction and oxidative stress are major contributors to the pathogenesis of AMD. Our findings highlight the need to elucidate how proline catabolism contributes to RPE metabolism *in vivo* and how it is influenced in diseased RPE cells.

Metabolite transport in RPE

Proline and its hydroxylated form, hydroxyproline, make up 25% of collagen (32), which is the most abundant protein in extracellular matrix (ECM) and in the collagenous zones of the Bruch membrane (BrM). The BrM is located between the RPE and the choroid, and ECM remodeling plays a critical role in the deposition of drusen in the BrM in AMD (33). Mutations of ECM metabolism genes have been identified in AMD patients (34). RPE cells control collagen synthesis for the BrM (35). Both [^{14}C]proline and [^3H]proline were incorporated in newly synthesized collagen in feline RPE cells and aged primate RPE cells (36, 37). In our preparations, RPE cells have abundant free hydroxyproline; however, it is not labeled by [^{13}C]proline in 1 h (Fig. 2B). This indicates that the hydroxylation of proline occurs after nascent collagen synthesis (38). It also suggests that the hydroxyproline turnover in collagen synthesis and degradation is a very slow process. Interestingly, one proline transporter, SLC6A20, is one of 154 RPE signature genes that is specifically and highly expressed in human RPE by a comparative study of gene expression from 78 tissues (39). Additional investigations will be required to show how carbons from proline are distributed to various metabolic pathways, how proline is transported, and how deprivation of proline in culture impacts RPE differentiation and function.

Besides proline, RPE also consumes substantial amounts of taurine and glucose. Photoreceptors are enriched with taurine, and they use glucose for aerobic glycolysis. RPE expresses glucose transporters and taurine transporters and is enriched with these two nutrients (10, 40, 41). Taurine supplementation promotes RPE proliferation and suppresses cell death in RPE culture (42, 43). As a well-known essential nutrient source, glucose is included in almost all RPE culture protocols. Deprivation of glucose reduces RPE viability, and attempts to rescue glucose-deprived RPE using other energy substrates have not been successful (20). These reports are consistent with our finding that the RPE needs these two basic nutrients under standard culture conditions.

We found that RPE cells export metabolic intermediates other than lactate and β -hydroxybutyrate into the culture medium. Citrate, glutamate, and glutamine are predominantly enriched in the culture medium on the apical side. Little is known about plasma membrane transporters for citrate and glutamine in RPE. Glutamate transporters have been found in cultured RPE cells, but their distribution is unknown (44, 45). Citrate is a key component of the TCA cycle, an important substrate for lipid biosynthesis, and a chelator for divalent cations like Ca^{2+} , Zn^{2+} , Fe^{2+} , and Mg^{2+} (46). Citrate is produced in the mitochondria and exported into the cytosol through the mitochondrial citrate transporter (SLC25a1). Alternatively, citrate can also be synthesized in the cytosol from αKG through reductive carboxylation by isocitrate dehydrogenase 1 (47). Three citrate transporters (SLC13A2, SLC13A3, and SLC13A5) are responsible for intracellular citrate transport or for import of citrate from blood (48). The citrate concentration in cerebrospinal fluid is about 0.4 mM (49). ^{13}C NMR spectroscopy has shown that astrocytes, but not neurons, are capable of exporting citrate (46, 49). Microvilli from the RPE surround photoreceptors outer segments. Photoreceptor uptake of citrate derived from the RPE might facilitate glycolysis by supplying

oxaloacetate to shuttle reducing power into mitochondria, provide acetyl-CoA for fatty acid synthesis, be utilized directly for the TCA cycle, and/or regulate divalent cations in the outer segment. Our RPE/retina co-culture experiments showing increased lactate, pyruvate, αKG , and glutamine in the mouse retina (Fig. 6E) support this hypothesis.

In the retina, glutamine is synthesized in glia cells and transported into photoreceptors to generate glutamate. We have reported a neuron-glia metabolism model in which lactate, together with neuron-derived aspartate, is used for glutamine synthesis in Müller cells in the retina (50). Our RPE/retina co-culture experiments revealed increased labeled glutamine in the retina and the apical medium with no change in RPE cells. Under our culture conditions, it appears that lactate produced either by the RPE or by photoreceptors in the retina contributes to glutamine synthesis within Müller cells. Additionally, glutamate is depleted from the apical medium when retina is present, suggesting that RPE cells might contribute to the glutamine-glutamate cycle.

Serine and glycine are synthesized from 3-phosphoglycerate, a glycolytic intermediate. Surprisingly, RPE causes an ~ 7 -fold increase in incorporation of ^{13}C from glucose into serine and glycine (Fig. 6E). Serine is used for biosynthesis of glycerophospholipids, sphingosine, and ceramide. These phospholipids are in high demand for the daily renewal of shed outer segments (51). Glycine is essential for purine biosynthesis. Purines like cGMP, ATP, and hypoxanthine are required for phototransduction (8). Additionally, metabolism of serine and glycine is an important source of NADPH, which is needed for anti-oxidative stress and lipid synthesis (52). Recent genome-wide analyses have shown that several key enzymes in the serine and glycine pathways have common variants associated with macular telangiectasia type 2, a neurovascular degenerative retinal disease (53).

In summary, we have shown that proline is a preferred nutrient source for cultured RPE cells. Proline is used to generate mitochondrial intermediates through both oxidative and reductive pathways. We found that RPE cells transport glucose-derived citrate, glutamate, serine, and glycine from their apical surface to be used by the retina. These findings reveal how RPE utilizes substrates and provide insights into RPE biochemistry and retinal diseases. It is important to note that we have shown in this study how RPE cells have these preferences when grown in culture. Additional experiments will be required to confirm that RPE cells in the eye of a live animal have similar preferences for metabolic fuels.

Experimental procedures

Reagents

Unless otherwise specified, all reagents were obtained from Sigma.

RPE cell culture

Human fetal RPE was isolated from fetal tissue (16–18 weeks of gestation) as reported previously (19, 26) and cultured for 4 weeks to form a confluent, pigmented monolayer of hexagonal cells. For nutrient transport experiments, RPE cells were passaged and grown on 0.4- μm transparent polyethylene tereph-

thylate membrane inserts (Corning, 353180) precoated with Matrigel (BD Biosciences) at 1×10^5 cells/insert for 4–6 weeks. The cells were cultured in RPE medium consisting of α minimum Eagle's medium (Life Technologies), non-essential amino acids (Life Technologies), N1 supplement (Life Technologies), 1% (v/v) FBS (Atlanta Biologicals), taurine, hydrocortisone, and triodo-thyronine (the detailed formulation of the medium can be found in supplemental Table 1). Transepithelial resistance (TER) was measured with a Millicell ERS-2 epithelial volt-ohm meter (Millipore). The pigmented RPE cells cultured on filter membranes with a TER ≥ 200 ohm/cm² were changed into 500 μ l of fresh RPE medium or DMEM with 1% FBS and [U-¹³C]glucose (Cambridge Isotope Laboratories Inc.) or [U-¹³C]proline. 20 μ l of medium was collected for metabolite analysis.

For the intracellular proline labeling experiments, RPE cells were cultured in precoated 6-well plates for 4–6 weeks. Prior to each experiment, the cells were changed into Krebs-Ringer bicarbonate buffer (KRB) (54) containing 5 mM glucose and 2 mM [U-¹³C]proline and incubated for 1 h before collection of medium and cells for metabolite analysis.

Retina and RPE co-culture

RPE cells grown on Millicell-HA filters (Millipore) for 4–6 weeks with TER ≥ 200 ohm/cm² were used for experiments. Isolated mouse retinas were laid on top of the RPE cells, with the photoreceptors facing the apical side of the RPE. Four cuts were made to the retina to relieve the curvature, and minimal medium was left in the apical chamber to make the retina flat. After 1 h, the medium was carefully changed into DMEM containing 1% FBS and 2 mM glutamine with unlabeled glucose on the apical side and [U-¹³C]glucose on the basal side.

Sample preparation for metabolite analysis

20 μ l of medium was mixed with 80 μ l of cold methanol on ice for 15 min to precipitate proteins. The mixture was centrifuged at 13,300 rpm for 15 min at 4 °C, and the supernatant was lyophilized for analysis by either LC/MS-MS or GC-MS. RPE cells, after removing the medium, were quickly rinsed with cold 0.9% NaCl and placed on dry ice to quench metabolism (54). 300 μ l of 80% (v/v) methanol was added to each well, and cells were scraped, homogenized, and spun down at 13,300 rpm at 4 °C for 15 min. The supernatant was dried for metabolite analysis, and the protein concentrations in the pellet were determined by BCA assay to normalize the metabolite data (54).

Metabolite analysis by LC/MS-MS

The LC/MS-MS method was described in detail previously (8, 55, 56). Briefly, dried metabolites were reconstituted in 200 μ l of 5 mM ammonium acetate in 95% water, 5% acetonitrile, and 0.5% acetic acid and filtered through 0.45- μ m PVDF filters. The metabolites were separated by a ethylene bridged hybrid Amid column (1.7 μ m, 2.1 mm \times 150 mm, Waters) with an Agilent 1260 LC (Agilent Technologies, Santa Clara, CA) and detected using an AB Sciex QTrap 5500 mass spectrometer (AB Sciex, Toronto, ON, Canada) system. Targeted data acquisition was performed in multiple reaction monitoring modes for 202 transitions listed in supplemental Table 2. The extracted peaks were integrated using MultiQuant 2.1 software (AB Sciex).

Metabolite analysis by GC-MS

All stable isotope-labeled metabolites were analyzed by GC-MS as reported previously (8, 19, 54). Dried samples were derivatized by methoxymine (Sigma) and *N*-tertbutyldimethylsilyl-*N*-methyltrifluoroacetamide (Sigma) and analyzed on an Agilent 7890/5975C GC-MS system (Agilent Technologies) using an HP-5MS column (30 m \times 0.25 mm \times 0.25 μ m, Agilent). The peaks were analyzed using Agilent Chemstation software, and the measured distribution of mass isotopomers was corrected for natural abundance with IsoCor software. Methylsuccinate was added to each sample as a reference. Enrichment was calculated by dividing the labeled ions by the total ion intensity.

Statistics

Data are expressed as the mean \pm S.D. The significance of differences between means was determined by unpaired two-tailed t tests or analysis of variance with an appropriate post hoc test. $p < 0.05$ was considered to be significant.

Author contributions—Conceptualization, J. R. C., J. B. H., and J. D.; Investigation, J. R. C., K. K., A. L. E., C. J., Y. W., M. A. M., H. G., D. D., D. R., and J. D.; Writing, J. D., J. B. H., and J. R. C.; Funding Acquisition, J. R. C., J. B. H., and J. D.; Supervision, J. R. C., J. B. H., and J. D.

Acknowledgments—We thank Dr. Martin Sadiliek, the director of the University of Washington Chemistry Mass Spectrometry Facility, for assistance with GC-MS analysis.

References

- Lehmann, G. L., Benedicto, I., Philp, N. J., and Rodriguez-Boulan, E. (2014) Plasma membrane protein polarity and trafficking in RPE cells: past, present and future. *Exp. Eye Res.* **126**, 5–15
- Strauss, O. (2005) The retinal pigment epithelium in visual function. *Physiol. Rev.* **85**, 845–881
- Sparrow, J. R., Hicks, D., and Hamel, C. P. (2010) The retinal pigment epithelium in health and disease. *Curr. Mol. Med.* **10**, 802–823
- Ambati, J., and Fowler, B. J. (2012) Mechanisms of age-related macular degeneration. *Neuron* **75**, 26–39
- Rattner, A., and Nathans, J. (2006) Macular degeneration: recent advances and therapeutic opportunities. *Nat. Rev. Neurosci.* **7**, 860–872
- Guziewicz, K. E., Sinha, D., Gómez, N. M., Zorych, K., Dutrow, E. V., Dhingra, A., Mullins, R. F., Stone, E. M., Gamm, D. M., Boesze-Battaglia, K., and Aguirre, G. D. (2017) Bestrophinopathy: an RPE-photoreceptor interface disease. *Prog. Retin. Eye Res.* **58**, 70–88
- Weber, B. H., Vogt, G., Pruett, R. C., Stöhr, H., and Felbor, U. (1994) Mutations in the tissue inhibitor of metalloproteinases-3 (TIMP3) in patients with Sorsby's fundus dystrophy. *Nat. Genet.* **8**, 352–356
- Du, J., Rountree, A., Cleghorn, W. M., Contreras, L., Lindsay, K. J., Sadilek, M., Gu, H., Djukovic, D., Raftery, D., Satrustegui, J., Kanow, M., Chan, L., Tsang, S. H., Sweet, I. R., and Hurley, J. B. (2016) Phototransduction influences metabolic flux and nucleotide metabolism in mouse retina. *J. Biol. Chem.* **291**, 4698–4710
- Hurley, J. B., Lindsay, K. J., and Du, J. (2015) Glucose, lactate, and shuttling of metabolites in vertebrate retinas. *J. Neurosci. Res.* **93**, 1079–1092
- Sugasawa, K., Deguchi, J., Okami, T., Yamamoto, A., Omori, K., Uyama, M., and Tashiro, Y. (1994) Immunocytochemical analyses of distributions of Na, K-ATPase and GLUT1, insulin and transferrin receptors in the developing retinal pigment epithelial cells. *Cell Struct. Funct.* **19**, 21–28
- Philp, N. J., Wang, D., Yoon, H., and Hjelmeland, L. M. (2003) Polarized expression of monocarboxylate transporters in human retinal pigment

- epithelium and ARPE-19 cells. *Invest. Ophthalmol. Vis. Sci.* **44**, 1716–1721
12. Philp, N. J., Ochrietor, J. D., Rudoy, C., Muramatsu, T., and Linser, P. J. (2003) Loss of MCT1, MCT3, and MCT4 expression in the retinal pigment epithelium and neural retina of the 5A11/basigin-null mouse. *Invest. Ophthalmol. Vis. Sci.* **44**, 1305–1311
 13. Ochrietor, J. D., and Linser, P. J. (2004) 5A11/Basigin gene products are necessary for proper maturation and function of the retina. *Dev. Neurosci.* **26**, 380–387
 14. Zhao, C., Yasumura, D., Li, X., Matthes, M., Lloyd, M., Nielsen, G., Ahern, K., Snyder, M., Bok, D., Dunaief, J. L., LaVail, M. M., and Vollrath, D. (2011) mTOR-mediated dedifferentiation of the retinal pigment epithelium initiates photoreceptor degeneration in mice. *J. Clin. Invest.* **121**, 369–383
 15. Kurihara, T., Westenskow, P. D., Gantner, M. L., Usui, Y., Schultz, A., Bravo, S., Aguilar, E., Wittgrove, C., Friedlander, M. S., Paris, L. P., Chew, E., Siuzdak, G., and Friedlander, M. (2016) Hypoxia-induced metabolic stress in retinal pigment epithelial cells is sufficient to induce photoreceptor degeneration. *eLife* **5**, e14319
 16. Maminishkis, A., Chen, S., Jalickee, S., Banzon, T., Shi, G., Wang, F. E., Ehalt, T., Hammer, J. A., and Miller, S. S. (2006) Confluent monolayers of cultured human fetal retinal pigment epithelium exhibit morphology and physiology of native tissue. *Invest. Ophthalmol. Vis. Sci.* **47**, 3612–3624
 17. Adijanto, J., and Philp, N. J. (2014) Cultured primary human fetal retinal pigment epithelium (hRPE) as a model for evaluating RPE metabolism. *Exp. Eye Res.* **126**, 77–84
 18. Johnson, L. V., Forest, D. L., Banna, C. D., Radeke, C. M., Maloney, M. A., Hu, J., Spencer, C. N., Walker, A. M., Tsie, M. S., Bok, D., Radeke, M. J., and Anderson, D. H. (2011) Cell culture model that mimics drusen formation and triggers complement activation associated with age-related macular degeneration. *Proc. Natl. Acad. Sci. U.S.A.* **108**, 18277–18282
 19. Du, J., Yanagida, A., Knight, K., Engel, A. L., Vo, A. H., Jankowski, C., Sadilek, M., Tran, V. T., Manson, M. A., Ramakrishnan, A., Hurley, J. B., and Chao, J. R. (2016) Reductive carboxylation is a major metabolic pathway in the retinal pigment epithelium. *Proc. Natl. Acad. Sci. U.S.A.* **113**, 14710–14715
 20. Wood, J. P., Chidlow, G., Graham, M., and Osborne, N. N. (2004) Energy substrate requirements of rat retinal pigmented epithelial cells in culture: relative importance of glucose, amino acids, and monocarboxylates. *Invest. Ophthalmol. Vis. Sci.* **45**, 1272–1280
 21. Fronk, A. H., and Vargis, E. (2016) Methods for culturing retinal pigment epithelial cells: a review of current protocols and future recommendations. *J. Tissue Eng.* **7**, 2041731416650838
 22. Maminishkis, A., and Miller, S. S. (2010) Experimental models for study of retinal pigment epithelial physiology and pathophysiology. *J. Vis. Exp.* **2032** 10.3791/2032
 23. Hu, J., and Bok, D. (2001) A cell culture medium that supports the differentiation of human retinal pigment epithelium into functionally polarized monolayers. *Mol. Vis.* **7**, 14–19
 24. Gamm, D. M., Melvan, J. N., Shearer, R. L., Pinilla, I., Sabat, G., Svendsen, C. N., and Wright, L. S. (2008) A novel serum-free method for culturing human prenatal retinal pigment epithelial cells. *Invest. Ophthalmol. Vis. Sci.* **49**, 788–799
 25. Akrami, H., Soheili, Z. S., Khalooghi, K., Ahmadi, H., Rezaie-Kanavi, M., Samiei, S., Davari, M., Ghaderi, S., and Sanie-Jahromi, F. (2009) Retinal pigment epithelium culture: a potential source of retinal stem cells. *J. Ophthalmic. Vis. Res.* **4**, 134–141
 26. Sonoda, S., Spee, C., Barron, E., Ryan, S. J., Kannan, R., and Hinton, D. R. (2009) A protocol for the culture and differentiation of highly polarized human retinal pigment epithelial cells. *Nat. Protoc.* **4**, 662–673
 27. Oka, M. S., Landers, R. A., and Bridges, C. D. (1984) A serum-free defined medium for retinal pigment epithelial cells. *Exp. Cell Res.* **154**, 537–547
 28. O'Donnell, J. J., Sandman, R. P., and Martin, S. R. (1978) Gyrate atrophy of the retina: inborn error of L-ornithin:2-oxoacid aminotransferase. *Science* **200**, 200–201
 29. Wang, T., Milam, A. H., Steel, G., and Valle, D. (1996) A mouse model of gyrate atrophy of the choroid and retina: early retinal pigment epithelium damage and progressive retinal degeneration. *J. Clin. Invest.* **97**, 2753–2762
 30. Ueda, M., Masu, Y., Ando, A., Maeda, H., Del Monte, M. A., Uyama, M., and Ito, S. (1998) Prevention of ornithine cytotoxicity by proline in human retinal pigment epithelial cells. *Invest. Ophthalmol. Vis. Sci.* **39**, 820–827
 31. Ando, A., Ueda, M., Uyama, M., Masu, Y., Okumura, T., and Ito, S. (2000) Heterogeneity in ornithine cytotoxicity of bovine retinal pigment epithelial cells in primary culture. *Exp. Eye Res.* **70**, 89–96
 32. Phang, J. M., Liu, W., and Zabornyk, O. (2010) Proline metabolism and microenvironmental stress. *Annu. Rev. Nutr.* **30**, 441–463
 33. Fernandez-Godino, R., Pierce, E. A., and Garland, D. L. (2016) Extracellular matrix alterations and deposit formation in AMD. *Adv. Exp. Med. Biol.* **854**, 53–58
 34. Duvvari, M. R., van de Ven, J. P., Geerlings, M. J., Saksens, N. T., Bakker, B., Henkes, A., Neveling, K., del Rosario, M., Westra, D., van den Heuvel, L. P., Schick, T., Fauser, S., Boon, C. J., Hoyng, C. B., et al. (2016) Whole exome sequencing in patients with the cuticular drusen subtype of age-related macular degeneration. *PLoS ONE* **11**, e0152047
 35. Nita, M., Strzalka-Mrozik, B., Grzybowski, A., Mazurek, U., and Romaniuk, W. (2014) Age-related macular degeneration and changes in the extracellular matrix. *Med. Sci. Monit.* **20**, 1003–1016
 36. Li, W., Stramm, L. E., Aguirre, G. D., and Rockey, J. H. (1984) Extracellular matrix production by cat retinal pigment epithelium *in vitro*: characterization of type IV collagen synthesis. *Exp. Eye Res.* **38**, 291–304
 37. Hirata, A., and Feeney-Burns, L. (1992) Autoradiographic studies of aged primate macular retinal pigment epithelium. *Invest. Ophthalmol. Vis. Sci.* **33**, 2079–2090
 38. Mitsubuchi, H., Nakamura, K., Matsumoto, S., and Endo, F. (2008) Inborn errors of proline metabolism. *J. Nutr.* **138**, 2016S-2020S
 39. Strunnikova, N. V., Maminishkis, A., Barb, J. J., Wang, F., Zhi, C., Sergeev, Y., Chen, W., Edwards, A. O., Stambolian, D., Abecasis, G., Swaroop, A., Munson, P. J., and Miller, S. S. (2010) Transcriptome analysis and molecular signature of human retinal pigment epithelium. *Hum. Mol. Genet.* **19**, 2468–2486
 40. Hillenkamp, J., Hussain, A. A., Jackson, T. L., Constable, P. A., Cunningham, J. R., and Marshall, J. (2004) Compartmental analysis of taurine transport to the outer retina in the bovine eye. *Invest. Ophthalmol. Vis. Sci.* **45**, 4099–4105
 41. El-Sherbeny, A., Naggar, H., Miyachi, S., Ola, M. S., Maddox, D. M., Martin, P. M., Ganapathy, V., and Smith, S. B. (2004) Osmoregulation of taurine transporter function and expression in retinal pigment epithelial, ganglion, and Muller cells. *Invest. Ophthalmol. Vis. Sci.* **45**, 694–701
 42. Gabrielian, K., Wang, H. M., Ogden, T. E., and Ryan, S. J. (1992) *In vitro* stimulation of retinal pigment epithelium proliferation by taurine. *Curr. Eye Res.* **11**, 481–487
 43. Udawatte, C., Qian, H., Mangini, N. J., Kennedy, B. G., and Ripps, H. (2008) Taurine suppresses the spread of cell death in electrically coupled RPE cells. *Mol. Vis.* **14**, 1940–1950
 44. Mäenpää, H., Gegelashvili, G., and Tähti, H. (2004) Expression of glutamate transporter subtypes in cultured retinal pigment epithelial and retinoblastoma cells. *Curr. Eye Res.* **28**, 159–165
 45. Miyamoto, Y., and Del Monte, M. A. (1994) Na⁺-dependent glutamate transporter in human retinal pigment epithelial cells. *Invest. Ophthalmol. Vis. Sci.* **35**, 3589–3598
 46. Westergaard, N., Waagepetersen, H. S., Belhage, B., and Schousboe, A. (2017) Citrate, a ubiquitous key metabolite with regulatory function in the CNS. *Neurochem. Res.* **42**, 1583–1588
 47. Jiang, L., Boufersaoui, A., Yang, C., Ko, B., Rakheja, D., Guevara, G., Hu, Z., and DeBerardinis, R. J. (2016) Quantitative metabolic flux analysis reveals an unconventional pathway of fatty acid synthesis in cancer cells deficient for the mitochondrial citrate transport protein. *Metab Eng.* **10.1016/j.ymben.2016.11.004**
 48. Pajor, A. M. (2014) Sodium-coupled dicarboxylate and citrate transporters from the SLC13 family. *Pflugers Arch* **466**, 119–130
 49. Sonnewald, U., Westergaard, N., Krane, J., Unsgård, G., Petersen, S. B., and Schousboe, A. (1991) First direct demonstration of preferential release of citrate from astrocytes using [13C]NMR spectroscopy of cultured neurons and astrocytes. *Neurosci. Lett.* **128**, 235–239

50. Lindsay, K. J., Du, J., Sloat, S. R., Contreras, L., Linton, J. D., Turner, S. J., Sadilek, M., Satrústegui, J., and Hurley, J. B. (2014) Pyruvate kinase and aspartate-glutamate carrier distributions reveal key metabolic links between neurons and glia in retina. *Proc. Natl. Acad. Sci. U.S.A.* **111**, 15579–15584
51. Ruggiero, L., and Finnemann, S. C. (2014) Lack of effect of microfilament or microtubule cytoskeleton-disrupting agents on restriction of externalized phosphatidylserine to rod photoreceptor outer segment tips. *Adv. Exp. Med. Biol.* **801**, 91–96
52. Ducker, G. S., and Rabinowitz, J. D. (2017) One-carbon metabolism in health and disease. *Cell Metab.* **25**, 27–42
53. Scerri, T. S., Quaglieri, A., Cai, C., Zernant, J., Matsunami, N., Baird, L., Schepke, L., Bonelli, R., Yannuzzi, L. A., Friedlander, M. S., Egan, C. A., Fruttiger, M., Leppert, M., Allikmets, R., and Bahlo, M. (2017) Genome-wide analyses identify common variants associated with macular telangiectasia type 2. *Nat. Genet.* **49**, 559–567
54. Du, J., Linton, J. D., and Hurley, J. B. (2015) Probing metabolism in the intact retina using stable isotope tracers. *Methods Enzymol.* **561**, 149–170
55. Zhu, J., Djukovic, D., Deng, L., Gu, H., Himmati, F., Chiorean, E. G., and Raftery, D. (2014) Colorectal cancer detection using targeted serum metabolic profiling. *J. Proteome Res.* **13**, 4120–4130
56. Gu, H., Carroll, P. A., Du, J., Zhu, J., Neto, F. C., Eisenman, R. N., and Raftery, D. (2016) Quantitative method to investigate the balance between metabolism and proteome biomass: starting from glycine. *Angew. Chem. Int. Ed. Engl.* **55**, 15646–15650

Supplemental Materials

Supplemental Method

Transmission electron microscopy of RPE/filter complex. RPE cultured on PET filter membranes for 4-6 weeks were fixed in half-strength Karnovsky's Fixative (2.5% glutaraldehyde, 2% formaldehyde in 0.1M buffer) for several days. Fixative was rinsed away with sodium cacodylate buffer. The scaffolds were stained with 2% osmium tetroxide for 1 hour, rinsed, and taken through a 30% to 100% ethanol dehydration series and two changes of propylene oxide. Dehydrated samples were embedded in EPON18+Araldite 502 (Electron Microscopy Sciences) before being cured for 24 hours at 60°C. Ultrathin (80 nm) sections were contrasted with lead citrate after being placed on copper grids for imaging with a JEOL JEM 1200EXII at 80 kV and a spot size of 3.

Supplemental Figure legends

Supplemental Table 1. Detected metabolites by LC MS in hfRPE culture medium

Supplemental Table 2. The formulation of RPE Medium

Supplemental Table 3. Metabolites in the apical and basal compartments in the absence of RPE cells

Supplemental Figure 1. Transmission electron microscopy (TEM) confirms polarity of RPE cells cultured on filter membranes. (A) RPE form microvilli at their apical surface (arrow; scale bar = 1µm) as well as (B) infoldings (arrow; scale bar = 0.5µm) on the basal side attached to the filter membrane (asterisk). (C) They also form tight junctions (arrow; scale bar = 1µm), which can be monitored by measuring transepithelial resistance.

Supplemental Figure 2. RPE consumes ¹³C labeled proline in the medium. RPE cells were cultured in KRB containing 5 mM glucose and 2mM ¹³C proline for 1 h. Medium metabolites were analyzed by GC MS. The intensity of ¹³C proline was normalized to the medium at 0 h. N=3, *P<0.05 vs the medium at 0h.

Supplemental Figure 3. Distribution of glucose-derived serine and glycine in the apical and basal side. (A-C). fRPE was cultured on filter with 500 µl of DMEM containing 2 mM glutamine and 1% FBS on each side with U-¹³C glucose at the apical side and glucose at the basal side. The ¹³C labeled serine and glycine in the medium from the apical and basal side. (D-F). The ¹³C labeled serine and glycine in the medium when U-¹³C glucose at the basal side. N=3.

Supplemental Figure 4. Rotenone does not cause RPE cell death. After 8 h incubation with 100 nM rotenone or 500 uM hydrogen peroxide as positive control, the medium was tested for LDH activity. The data were normalized by the medium from the control. N=3. NS, no significance vs Con; *P<0.05 vs Con.

Supplemental Table 1. Formulation of RPE medium

Components	Concentration (mg/L)	mM	Category	Source
Glycine	57.5	0.7667	Amino Acids	MEM alpha + NEAA
L-Alanine	33.9	0.3809	Amino Acids	MEM alpha + NEAA
L-Arginine hydrochloride	105	0.4976	Amino Acids	MEM alpha
L-Asparagine-H ₂ O	63.2	0.4333	Amino Acids	MEM alpha + NEAA
L-Aspartic acid	43.3	0.3256	Amino Acids	MEM alpha + NEAA
L-Cysteine hydrochloride-H ₂ O	100	0.5682	Amino Acids	MEM alpha
L-Cystine 2HCl	31	0.0990	Amino Acids	MEM alpha
L-Glutamic Acid	89.8	0.6102	Amino Acids	MEM alpha + NEAA
L-Glutamine	292	2.0000	Amino Acids	MEM alpha
L-Histidine hydrochloride-H ₂ O	42	0.2000	Amino Acids	MEM alpha
L-Isoleucine	52.4	0.4000	Amino Acids	MEM alpha
L-Leucine	52	0.3969	Amino Acids	MEM alpha
L-Lysine hydrochloride	73	0.3989	Amino Acids	MEM alpha
L-Methionine	15	0.1007	Amino Acids	MEM alpha
L-Phenylalanine	32	0.1939	Amino Acids	MEM alpha
L-Proline	51.5	0.4478	Amino Acids	MEM alpha + NEAA
L-Serine	35.5	0.3381	Amino Acids	MEM alpha + NEAA
L-Threonine	48	0.4034	Amino Acids	MEM alpha
L-Tryptophan	10	0.0490	Amino Acids	MEM alpha
L-Tyrosine disodium salt	52	0.1985	Amino Acids	MEM alpha
L-Valine	46	0.3932	Amino Acids	MEM alpha
Ascorbic Acid	50	0.2841	Vitamins	MEM alpha
Biotin	0.1	0.0004	Vitamins	MEM alpha
Choline chloride	1	0.0071	Vitamins	MEM alpha
D-Calcium pantothenate	1	0.0021	Vitamins	MEM alpha
Folic Acid	1	0.0023	Vitamins	MEM alpha
Niacinamide	1	0.0082	Vitamins	MEM alpha
Pyridoxal hydrochloride	1	0.0049	Vitamins	MEM alpha
Riboflavin	0.1	0.0003	Vitamins	MEM alpha

Thiamine hydrochloride	1	0.0030	Vitamins	MEM alpha
Vitamin B12	1.36	0.0010	Vitamins	MEM alpha
i-Inositol	2	0.0111	Vitamins	MEM alpha
Calcium Chloride (CaCl ₂) (anhyd.)	200	1.8018	Inorganic Salts	MEM alpha
Magnesium Sulfate (MgSO ₄) (anhyd.)	97.67	0.8139	Inorganic Salts	MEM alpha
Potassium Chloride (KCl)	400	5.3333	Inorganic Salts	MEM alpha
Sodium Bicarbonate (NaHCO ₃)	2200	26.1905	Inorganic Salts	MEM alpha
Sodium Chloride (NaCl)	6800	117.2414	Inorganic Salts	MEM alpha
Sodium Phosphate monobasic (NaH ₂ PO ₄ -H ₂ O)	140	1.0145	Inorganic Salts	MEM alpha
D-Glucose (Dextrose)	1000	5.5556	Other components	MEM alpha
Lipoic Acid	0.2	0.0010	Other components	MEM alpha
Phenol Red	10	0.0266	Other components	MEM alpha
Sodium Pyruvate	110	1.0000	Other components	MEM alpha
Recombinant human insulin	5		Other components	N1 Supplement
human transferrin	5		Other components	N1 Supplement
Sodium selenite	0.005		Other components	N1 Supplement
Putrescine	16		Other components	N1 Supplement
Progesterone	0.0073		Other components	N1 Supplement
Taurine	250			Supplement
Hydrocortisone	0.02			Supplement
triiodo-thyronine	0.000013			Supplement
Fetal Bovine Serum	1% (V/V)			Supplement

Supplemental Table 2. The detected metabolites by LC MS in hFRPE culture medium

Metabolite	Q1/Q3	CAS	Metabolic pathways	Detected
1-Methyladenosine	282.0 / 150.1	15763-06-1	Nucleotide/Purine metabolism	Yes
2-Amino adipate	160.1 / 116.0	542-32-5	Amino acids metabolism/Lys	Yes
2-Hydroxyglutarate	147.0 / 129.0	63512-50-5	Amino-acid metabolism & Glycine/Serine/Threonine metabolism	Yes
2-Hydroxyisovaleric Acid	117.0 / 71.0	625-08-1	Amino Acid	Yes
3HBA	103.0 / 59.0	625-72-9	TCA Cycle	Yes
3-Methyl-2-Oxovaleric Acid	129.0 / 101.0	1460-34-0	Amino Acid	Yes
4-Hydroxybutyrate	105.0 / 77.0	591-81-1	Lipids/phospholipids, ligand	Yes
4-Pyridoxic acid	182.1 / 138.0	82-82-6	Vitamins/B6	Yes
5-Aminovaleric Acid	118.0 / 55.0	660-88-8	Amino Acid	Yes
Acetoacetate	101.0 / 57.0	541-50-4	Ketone	Yes
Acetylcarnitine	204.1 / 85.0	3040-38-8	Fatty acid Oxidation	Yes
Acetylcholine	146.1 / 87.0	60-32-1	Lipids/phospholipids, ligand	Yes
Aconitate	173.0 / 85.0	4023-65-8	TCA Cycle	Yes
Adenosine	268.1/136.1	58-61-7	Nucleotide/Purine metabolism	Yes
Adipic Acid	144.9 / 83.0	124-04-9	Caprolactam degradation	Yes
Agmanite	131.0 / 72.0	2482-00-0	Polyamine metabolism	Yes
Alanine	90.0 / 44.0	56-41-7	Amino Acid	Yes
Alpha-Ketoglutaric Acid	145.0 / 101.0	328-50-7	TCA Cycle	Yes
Anthranilate	136.0 / 118.0	118-92-3	Amino Acid metabolism/Trp, Phe, Tyr	Yes
Arachidonate	303.3 / 59.0	6610-25-9	Lipids/phospholipids, ligand	Yes
Arginine	175.1 / 70.0	1119-34-2	Amino Acid	Yes
Asparagine	133.1 / 74.0	70-47-3	Amino Acid	Yes
Aspartic Acid	134.1 / 74.0	56-84-8	Amino Acids	Yes
Azelaic Acid	187.0 / 125.0	123-99-9	Fatty Acids and Conjugates	Yes
Benzoic acid	121.0 / 77.0	65-85-0	Amino Acid (Phenylalanine Metabolism, others)	Yes
Betaine	118.0 / 58.0	107-43-7	Amino acids metabolism /Gly,Ser, Thr metabolism	Yes
Biotin	243.1 / 200.0	58-85-5	Vitamins	Yes
Carnitine	162.1 / 85.0	541-15-1	Amino acids metabolism /Lys	Yes
Chenodeoxycholate	391.0 / 74.0	474-25-9	Bile acid metabolism	Yes
Choline	104.1 / 60.0	62-49-7	Vitamins	Yes

Citraconic Acid	129.0 / 85.0	498-23-7	Amino Acid metabolism /Val, Leu, IL	Yes
Citric Acid	191.0 / 111.0	77-92-9	TCA Cycle	Yes
Citrulline	174.0 / 131.0	372-75-8	Urea Cycle	Yes
Creatine	132.1 / 90.0	57-00-1	Amino acids metabolism /Arg, Gly	Yes
Cystathionine	221.1 / 134.0	56-88-2	Amino acids metabolism /cys	Yes
Cysteine	122.0 / 59.0	52-90-4	Amino Acid	Yes
Cystine	241.1 / 120.0	56-89-3	Amino acids metabolism	Yes
Cytidine	244.0 / 112.1	65-46-3	Nucleotide/Pyrimidine metabolism	Yes
Deoxycarnitine	147.1 / 87.0	6249-56-5	Lipids/phospholipids, ligand	Yes
D-Leucic Acid	131.0 / 85.0	20312-37-2	Amino Acid metabolism/Leu	Yes
Dopamine	152.1 / 122.0	62-31-7	Adrenaline Metabolism	Yes
Epinephrine/Normetanephrine	184.1 / 166.2	51-43-4	Amino Acid metabolism /Tyr,ligand	Yes
Erythrose	119.0 / 71.0	1758-51-6	Sugar	Yes
F16BP/F26BP/G16BP	339.0 / 97.0	488-69-7	Glycolysis/sugar	Yes
Folic Acid	440.1 / 311.0	59-30-3	One carbon pool by folate	Yes
Fumaric Acid	115.0 / 71.0	100-17-8	TCA Cycle	Yes
G6P/F6P/F1P	259.0 / 97.0	56-73-5	Glycolysis/sugar	Yes
gama-Aminobutyrate	102.1 / 56.0	56-12-2	Amino Acid metabolism /Ala, Glu, Asp	Yes
Glucose	179.0 / 89.0	50-99-7	Glycolysis/sugar	Yes
Glutamic acid	148.1 / 84.0	56-86-0	Amino Acid	Yes
Glutamine	147.1 / 84.0	56-85-9	Amino Acid	Yes
Glutaric Acid	131.0 / 87.0	110-94-1	Amino Acids/lys, trp, fatty acids	Yes
Glyceraldehyde	89.0 / 59.0	56-82-6	Sugar	Yes
Glycerate	105.0 / 75.0	600-19-1	Amino Acid metabolism /Gly, Ser	Yes
Glycine	76.0 / 30.1	56-40-6	Amino Acid	Yes
Guanosine	284.0 / 152.1	118-00-3	Nucleotide/Purine metabolism	Yes
Histidine	156.1 / 110.0	5934-29-2	Amino Acid	Yes
Homoserine	120.1 / 74.0	672-15-1	Amino acids metabolism /Thr, Met, Asp	Yes
Homovanilate	181.0 / 137.0	306-08-1	Amino acids metabolism /Tyr,ligand	Yes
Hydroxyproline	132.1 / 86.2	51-35-4	Amino acids metabolism /Pro	Yes
Hypoxanthine	135.0 / 92.0	68-94-0	Nucleotide	Yes

Inosine	269.0 / 137.1	58-63-9	Nucleotide/Purine metabolism	Yes
Inositol	179.0 / 87.0	87-89-8	Glucose/inositol metabolism	Yes
iso-Leucine	132.1 / 86.0	73-32-5	Amino Acid	Yes
isoValeric Acid	101.0 / 83.0	503-74-2	Amino Acid	Yes
Kynurenate	188.0 / 143.8	492-27-3	Amino Acid metabolism /Try	Yes
lactate	89.0 / 43.0	79-33-4	Glycolysis/TCA	Yes
Lactose	341.0 / 59.0	63-42-3	Sugar/Galactose	Yes
Leucine	132.1 / 86.0	61-90-5	Amino Acid	Yes
L-Kynurenine	209.1 / 94.0	343-65-7	Tryptophan Cycle	Yes
Lysine	147.1 / 84.0	56-87-1	Amino Acid	Yes
Malate	133.0 / 115.0	6915-15-7	TCA Cycle	Yes
Maleic Acid	115.0 / 71.0	110-16-7	TCA Cycle	Yes
Malonic Acid	103.0 / 41.0	141-82-2	TCA Cycle	Yes
Margaric Acid	269.1 / 251.3	506-12-7	Fatty acid metabolism	Yes
Methionine	150.1 / 61.0	63-68-3	Amino Acid	Yes
Myristic Acid	227.1 / 209.0	544-63-8	Fatty acid metabolism	Yes
N2,N2-Dimethylguanosine	312.0 / 180.1	2140-67-2	Nucleotide/Purine metabolism	Yes
N-AcetylGlycine	116.0 / 74.0	543-24-8	Amino Acid metabolism	Yes
Niacinamide	123.0 / 80.0	98-92-0	Vitamins	Yes
OH-Phenylpyruvate	179.0 / 89.0	156-39-8	Amino Acid / Tyrosine metabolism	Yes
Ornithine	133.1 / 70.0	3184-13-2	Urea cycle	Yes
Orotate	155.0 / 111.0	50887-69-9	Nucleotide/Pyrimidine metabolism	Yes
Oxalacetate	131.0 / 113.0	328-42-7	TCA Cycle	Yes
Pentothenate	218.1 / 88.0	137-08-6	Amino acids metabolism /alanine, CoA	Yes
Phenylalanine	166.1 / 120.0	63-91-2	Amino Acid	Yes
Pipecolate	130.0 / 84.0	3105-95-1	Amino Acid	Yes
Proline	116.1 / 70.0	147-85-3	Amino Acid	Yes
Putrescine	89.0 / 72.0	110-60-1	Polyamine metabolism	Yes
Pyroglutamic Acid	130.0 / 83.4	98-79-3	Amino acids/Glu	Yes
Pyruvate	87.0 / 43.0	127-17-3	Glycolysis/amino acids metabolism	Yes
Quinolate	166.0 / 78.0	89-00-9	Amino Acid/ Tryptophan, alanine metabolism	Yes
Ribose-5-P	229.0 / 79.0	3615-55-2	Pentose phosphate pathway	Yes
Salicylurate	196.1 / 152.0	487-54-7	Amino Acid metabolism /Gly	Yes
Sarcosine	89.9 / 44.0	107-97-1	Amino Acid	Yes
Serine	106.0 / 60.0	56-45-1	Amino Acid	Yes

Shikimic Acid	173.0 / 93.0	138-59-0	Amino Acid metabolism /Phe, Tyr,Trp	Yes
Sorbitol	183.0 / 91.0	6706-59-8	Sugar	Yes
Spermidine	146.1 / 72.0	124-20-9	Polyamine metabolism	Yes
Succinate	117.0 / 73.0	110-15-6	TCA Cycle	Yes
Sucrose	341.0 / 59.0	57-50-1	Sugar	Yes
Taurine	126.0 / 108.0	107-35-7	Amino acids metabolism/Sulfur metabolism	Yes
Threonine	120.1 / 74.0	72-19-5	Amino Acid	Yes
Trimethylamine-N-oxide (TMAO)	76.1 / 58.0	1184-78-7	Gut flora metabolism / Redox	Yes
Tryptophan	205.1 / 146.0	73-22-3	Tryptophan Cycle	Yes
Tyrosine	182.1 / 136.0	60-18-4	Amino Acid	Yes
Uridine	245.0 / 113.1	58-96-8	Nucleotide/Pyrimidine metabolism	Yes
Valine	118.1 / 72.0	72-18-4	Amino Acid	Yes
Xanthine	151.0 / 108.0	69-89-6	Nucleotide	Yes
Xanthurenate	204.0 / 160.0	59-00-7	Amino acids metabolism	Yes
1/3-Methylhistidine	170.0 / 96.0	368-16-1	Amino Acid (Histidine Metabolism)	
12-HETE	319.2 / 179.0	54397-83-0	Lipids/phospholipids, ligand	
13-HODE	295.2 / 195.0	29623-28-7	Lipids/phospholipids, ligand	
1-Methylguanosine	298.0 / 166.1	2140-65-0	Nucleotide/Purine metabolism	
1-Methylhistamine	126.0 / 96.0	501-75-7	Amino acids metabolism/His	
3-Phosphoglyceric Acid	185.0 / 97.0	820-11-1	Glycolysis	
2'-Deoxyuridine	229.0 / 113.0	951-78-0	Nucleotide/Pyrimidine metabolism	
3-Hydroxykynurenine	225.2 / 110.1	484-78-6	Tryptophan Cycle	
3-Nitro-tyrosine	225.0 / 163.0	3604-79-3	Oxidative Damage	
5-Hydroxymethyl-2'-deoxyuridine	259.0 / 143.1	5116-24-5	Nucleotide/Purine metabolism	
5-Hydroxytryptophan	221.0 / 133.2	4530-09-8	Tryptophan Cycle	
6-Methyladenosine	282.0 / 150.1	1867-73-8	Nucleotide/Purine metabolism	
8-hydroxyguanosine	300.0 / 168.1	3868-31-3	Nucleotide/Purine metabolism	
8-Oxo-2'-deoxyguanosine	284.0 / 168.1	88847-89-6	Nucleotide/Purine metabolism	
Adenine	134.1 / 107.0	73-24-5	Nucleotide/Purine metabolism	
Adenylosuccinate	462.1 / 79.0	19046-78-7	Nucleotide/Purine metabolism	

ADP	426.0 / 134.0	20398-34-9	Nucleotide/Purine metabolism	
Allantoin	157.0 / 114.0	97-59-6	Nucleotide Degradation	
Allopurinol	135.0 / 64.0	315-30-0	Nucleotide metabolism (Drug)	
Aminoisobutyrate	104.1 / 86.0	144-90-1	Amino acids metabolism /Val, Leu, iso-Leu	
AMP	346.1 / 79.0	149022-20-8	Nucleotide	
Ascorbic Acid (Vit. C)	175.0 / 87.0	50-81-7	Vitamin, Cofactor	
ATP	505.9 / 79.0	51963-61-2	Nucleotide	
Cadaverine	103.0 / 86.0	462-94-2	Amino Acid	
cGMP	344.0 / 150.0	7665-99-8	Nucleotide/Purine metabolism	
CMP	322.0 / 97.0	63-37-6	Nucleotide/Pyrimidine metabolism	
Creatinine	114.1 / 44.0	60-27-5	Amino acids metabolism /Arg, Gly	
Cystamine	153.0 / 108.0	51-85-4	Amino acids metabolism /Cys	
Cysteinyl-Glycine (Cys-Gly)	179.1 / 76.0	19246-18-5	Amino acids degradation	
Cytosine	112.1 / 95.0	71-30-7	Nucleotide	
DCDP	386.0 / 159.0	800-73-7	Nucleotide/Pyrimidine metabolism	
DCMP	306.0 / 110.0	1032-65-1	Nucleotide/pyrimidine	
D-GA3P	168.9 / 97.0	142-10-9	Glycolysis/Glycogenesis	
DHAP	168.9 / 78.8	57-04-5	Glycolysis/phospholipid	
Dimethylglycine	104.1 / 58.0	1118-68-9	Vitamins	
DTMP	321.1 / 79.0	365-07-1	Nucleic Acid	
DUMP	307.0 / 195.0	964-26-1	Nucleotide/pyrimidine	
DUTP	467.0 / 159.0	1173-82-6	Nucleotide/pyrimidine	
Fructose	179.0 / 89.0	57-48-7	Sugar	
Galactose	179.0 / 89.0	15572-79-9	Sugars	
GDP	442.0 / 159.0	43139-22-6	Nucleotide/Purine metabolism	
Geranyl Pyrophosphate	313.1 / 79.1	763-10-0	Ubiquinone and other terpenoid-quinone biosynthesis	
Gibberellin	345.2 / 144.2	77-06-5	Diterpenoid biosynthesis	
Glucuronate	193.0 / 73.0	1700908	Amino sugar and nucleotide sugar metabolism	
Glucosamine	180.1 / 162.0	3416-24-8	Amino sugar and nucleotide sugar metabolism	
Glycerol	93.0 / 75.0	56-81-5	Fatty acid metabolism	

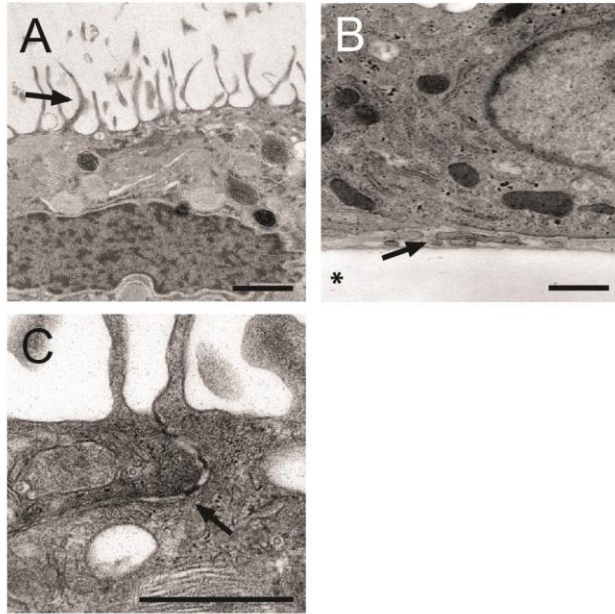
Glycerol-3-P	171.0 / 79.0	29849-82-9	Lipids/Glycerol lipid	
Glycochenodeoxycholate	448.3 / 74.0	640-79-9	Bile acid metabolism	
Glycocholate	464.3 / 74.0	475-31-0	Bile acid metabolism	
GMP	364.1 / 151.8	85-32-5	Nucleotide/Purine metabolism	
GTP	522.0 / 159.0	373-49-9	Nucleotide/Purine metabolism	
Guanidinoacetate	116.0 / 74.0	352-97-6	Amino Acid metabolism /Gly, Ser,Thr	
Histamine	112.0 / 95.0	51-45-6	Nucleotide	
Homocysteine	136.0 / 90.0	454-29-5	Amino acids metabolism /Cys, Met	
Homogentisate	167.0 / 123.0	451-13-8	Amino Acid metabolism /Tyr	
Hippuric Acid	178.0 / 134.0	495-69-2	Amino Acid metabolism /Gly	
IMP	347.0 / 79.0	131-99-7	Nucleotide/Purine metabolism	
isoButyric Acid	87.0 / 42.0	79-31-2	Fatty acid metabolism	
Linoleic Acid	277.1 / 259.0	60-33-3	Fatty acid metabolism	
Linolenic Acid	279.1 / 261.0	463-40-1	Fatty acid metabolism	
Malondialdehyde	71.0 / 41.0	542-78-9	Oxidative Damage	
Mannose	181.0 / 99.0	3458-28-4	Sugar/Galactose Metabolism	
Melatonin	231.1 / 58.0	73-31-4	Neuroactive ligand	
Methylmalonate	117.0 / 73.0	516-05-2	Vitamins	
Methyl-OH-isobutyrate	117.0 / 85.0	2110-78-3	Fatty acid metabolism	
MethylSuccinate	131.0 / 69.0	498-21-5	Amino Acid metabolism /Isoleu	
Mevalonate	147.1 / 59.0	150-97-0	Terpenoid backbone biosynthesis	
N-Acetylneuraminate	308.1 / 87.0	131-48-6	Sugars	
N-Acetylputrescine	131.1 / 114.0	18233-70-0	Polyamine metabolism	
N-Carbamoyl-B-Alanine	131.1 / 115.0	462-88-4	Urea cycle	
Nicotinate (Niacin)	122.0 / 78.0	59-67-6	Nicotinate and nicotinamide metabolism	
OMP	367.0 / 323.1	2149-82-8	Nucleotide/Pyrimidine metabolism	
Oxalic Acid	89.0 / 61.0	144-62-7	Glyoxylate and dicarboxylate metabolism	
Oxidized glutathione	611.2 / 306.0	27025-41-8	Oxidative Damage	
Oxypurinol	151.0 / 42.0	2465-59-0	Nucleotide metabolism	
PEP	166.9 / 79.0	138-08-9	Glycolysis	
PGE	351.2 / 315.3	363-24-6	Lipids/Arachidonic acid metabolism	
Phosphotyrosine	262.0 / 81.0	N/A	Amino acids metabolism	

PPA	163.0 / 91.0	156-06-9	Amino acids metabolism/Phe	
Propionate	73.0 / 55.0	79-09-4	Nicotinate and nicotinamide metabolism	
PRPP	389.0 / 176.9	7540-64-9	Nucleotide/Purine metabolism	
Pyridoxal-5-P	246.0 / 96.9	54-47-7	Vitamins/B6	
Reduced glutathione	306.1 / 143.0	70-18-8	Oxidative Damage	
Spermine	203.1 / 129.0	71-44-3	Polyamine metabolism	
Taurocholate	514.5 / 124.0	81-24-3	Conjugated bile acid biosynthesis	
Trimethylamine (TMA)	60.0 / 44.0	75-50-3	Gut flora metabolism / Redox	
Tryptamine	161.1 / 144.0	61-54-1	Amino Acid	
Tyramine	138.1 / 77.0	51-67-2	Amino Acid	
UDP	403.0 / 79.0	21931-53-3	Nucleotide/Pyrimidine metabolism	
Uracil	111.0 / 42.0	66-22-8	Nucleotide/Pyrimidine metabolism	
Urate	167.0 / 124.0	69-93-2	Nucleotide/Purine metabolism	
Xanthosine	283.1 / 151.0	146-80-5	Nucleotide/Purine metabolism	

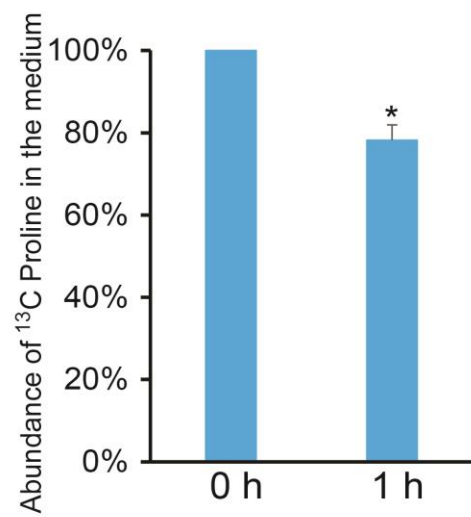
Supplemental Table 3. Metabolites from apical and basal side without RPE cells

Metabolite (Q1/Q3)	Apical	Basal	Basal/Apical
Deoxycarnitine (147.1 / 87.0)	108617	99340	-1.09
Orotate (155.0 / 111.0)	660670	595588	-1.11
Malate (133.0 / 115.0)	78580	71128	-1.10
Succinate (117.0 / 73.0)	479093	435979	-1.10
G1P/G6P/F6P/F1P (259.0 / 97.0)	26740	24607	-1.09
Choline (104.1 / 60.0)	74022501	68297218	-1.08
Tryptophan (205.1 / 146.0)	20997904	19399555	-1.08
Proline (116.1 / 70.0)	47939248	44459344	-1.08
D-Leucic Acid (131.0 / 85.0)	74664	69408	-1.08
Methionine (150.1 / 61.0)	21346013	19845649	-1.08
Pipecolate (130.0 / 84.0)	63759837	59336533	-1.07
2/3-Phosphoglyceric Acid (185.0 / 97.0)	142105	132805	-1.07
Leucine (132.1 / 86.0)	124332792	116285961	-1.07
Glycine (76.0 / 30.1)	1803654	1688284	-1.07
4-Hydroxybutyrate (105.0 / 77.0)	526124	492648	-1.07
Cystine (241.1 / 120.0)	23511115	22031136	-1.07
Serine (106.0 / 60.0)	38300307	35901714	-1.07
5-Aminovaleric Acid (118.0 / 55.0)	76442002	71658210	-1.07
Pentothenate (218.1 / 88.0)	36025024	33792298	-1.07
Ornithine (133.1 / 70.0)	949045	890298	-1.07
Phenylalanine (166.1 / 120.0)	158648320	149587484	-1.06
Glutamine (147.1 / 84.0)	139606038	131708750	-1.06
Sorbitol (183.0 / 91.0)	1647319	1557368	-1.06
Adipic Acid (144.9 / 83.0)	281842	266461	-1.06
2-Hydroxyglutarate (147.0 / 129.0)	1559846	1474924	-1.06
Agmanite (131.0 / 72.0)	231852	219491	-1.06
iso-Leucine (132.1 / 86.0 (2))	129931131	123169053	-1.05
Putrescine (89.0 / 72.0)	10714368	10178649	-1.05
Oxalacetate (131.0 / 113.0)	19802264	18837607	-1.05
Tyrosine (182.1 / 136.0)	41401807	39394375	-1.05
Anthranilate (136.0 / 118.0)	207168	197264	-1.05
isoValeric Acid (101.0 / 83.0)	1023726	974969	-1.05
Valine (118.1 / 72.0)	36690045	34944587	-1.05
Inositol (179.0 / 87.0)	3390301	3230416	-1.05
Erythrose (119.0 / 71.0)	311672	296983	-1.05
Pyroglutamic Acid (130.0 / 83.4)	2230801	2127104	-1.05
Betaine (118.0 / 58.0)	227800	217293	-1.05
Guanosine (284.0 / 152.1)	30152	28809	-1.05
Margaric Acid (269.1 / 251.3)	46066	44036	-1.05

Taurine (126.0 / 108.0)	291529	278804	-1.05
gama-Aminobutyrate (102.1 / 56.0)	51899	49700	-1.04
Alanine (90.0 / 44.0)	10362304	9927712	-1.04
Glycerate (105.0 / 75.0)	2364611	2276912	-1.04
Threonine (120.1 / 74.0 (2))	100265088	96631988	-1.04
Glutamic acid (148.1 / 84.0)	24329306	23523293	-1.03
Aspartic Acid (134.1 / 74.0)	10419145	10078003	-1.03
5-Hydroxytryptophan (221.0 / 133.2)	51444	49820	-1.03
Xanthurenate (204.0 / 160.0)	375778	366283	-1.03
Arachidonate (303.3 / 59.0)	313777	306517	-1.02
Alpha-Ketoglutaric Acid (145.0 / 101.0)	15699362	15367425	-1.02
Glutaric Acid (131.0 / 87.0)	97437	95613	-1.02
Lactose (341.0 / 59.0)	242351	238545	-1.02
Lysine (147.1 / 84.0 (2))	140535658	138939810	-1.01
Citrulline (174.0 / 131.0)	6205036	6137912	-1.01
Histidine (156.1 / 110.0)	88798120	88030618	-1.01
Sucrose (341.0 / 59.0 (2))	78008	77640	1.00
Homovanilate (181.0 / 137.0)	2278458	2272062	1.00
N-AcetylGlycine (116.0 / 74.0)	99550	99379	1.00
Arginine (175.1 / 70.0)	122727332	123515225	1.01
Glucose (179.0 / 89.0)	125734860	126835139	1.01
2-Hydroxyisovaleric Acid (117.0 / 71.0)	46543	47109	1.01
L-Kynurenine (209.1 / 94.0)	176495	179959	1.02
4-Pyridoxic acid (182.1 / 138.0)	6194403	6316381	1.02
Azelaic Acid (187.0 / 125.0)	1431051	1471069	1.03
3HBA (103.0 / 59.0)	389630	401492	1.03
Citraconic Acid (129.0 / 85.0)	156095	162246	1.04
Trimethylamine-N-oxide (TMAO) (76.1 / 58.0)	178383	186300	1.04
OH-Phenylpyruvate (179.0 / 89.0 (4))	150449	157250	1.05
lactate (89.0 / 43.0)	1115622	1175040	1.05
Asparagine (133.1 / 74.0)	6450226	6856641	1.06
Fumaric Acid (115.0 / 71.0)	377718	403619	1.07
F16BP/F26BP/G16BP (339.0 / 97.0)	423450	453034	1.07
3-Methyl-2-Oxovaleric Acid (129.0 / 101.0)	19146	20689	1.08
Nicotinate (Niacin) (122.0 / 78.0)	150644	162905	1.08
Niacinamide (123.0 / 80.0)	11649630	12621067	1.08
Shikimic Acid (173.0 / 93.0)	65286	70901	1.09
Kynurenate (188.0 / 143.8)	140534	156442	1.11
1C13-Lactate (90.0 / 44.0)	31854029	33764511	1.06
213C-Tyrosine (184.1 / 138.0)	48851901	50342024	1.03

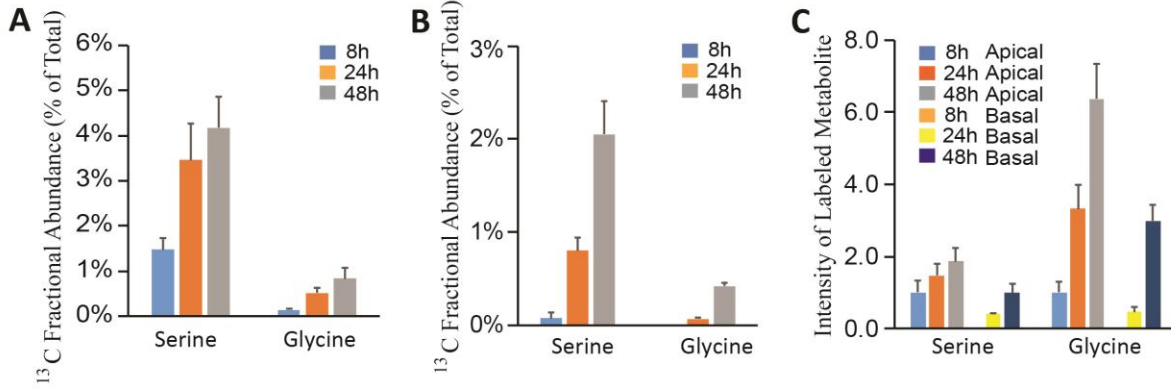


Supplemental Figure 1

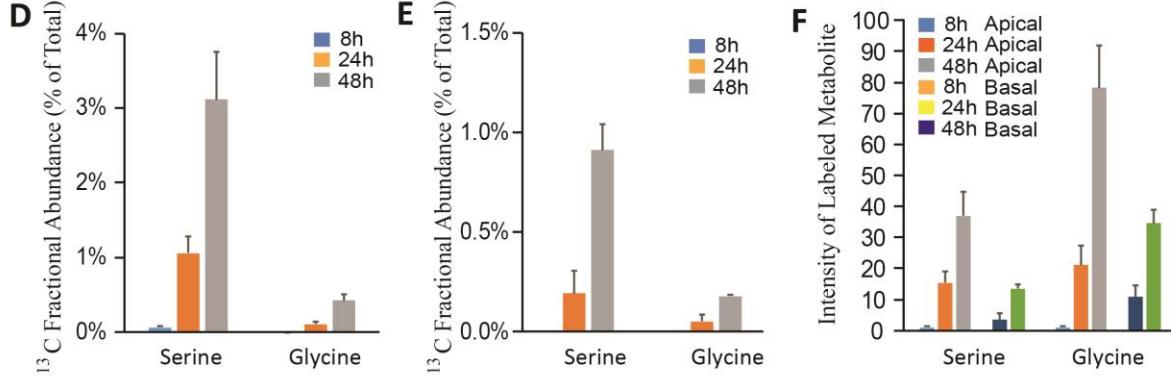


Supplemental Figure 2

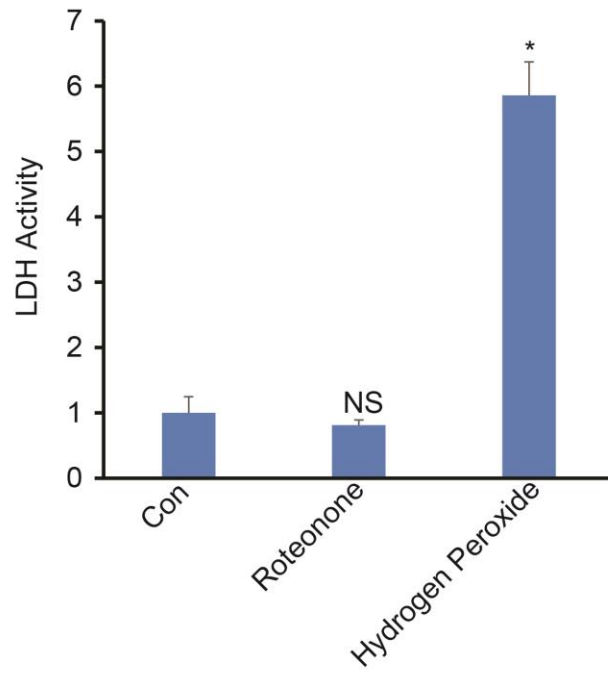
U-¹³C glucose is in the **apical** side



U-¹³C glucose is in the **basal** side



Supplemental Figure 3



Supplemental Figure 4

Human retinal pigment epithelial cells prefer proline as a nutrient and transport metabolic intermediates to the retinal side

Jennifer R. Chao, Kaitlen Knight, Abbi L. Engel, Connor Jankowski, Yekai Wang, Megan A. Manson, Haiwei Gu, Danijel Djukovic, Daniel Raftery, James B. Hurley and Jianhai Du

J. Biol. Chem. 2017, 292:12895-12905.

doi: 10.1074/jbc.M117.788422 originally published online June 14, 2017

Access the most updated version of this article at doi: [10.1074/jbc.M117.788422](https://doi.org/10.1074/jbc.M117.788422)

Alerts:

- [When this article is cited](#)
- [When a correction for this article is posted](#)

[Click here](#) to choose from all of JBC's e-mail alerts

Supplemental material:

<http://www.jbc.org/content/suppl/2017/06/14/M117.788422.DC1>

This article cites 56 references, 17 of which can be accessed free at <http://www.jbc.org/content/292/31/12895.full.html#ref-list-1>